San Jose State University
Foundation
One Washington Sq. P.O.Box 760
San Jose, Ca 95106

NCC 2-466

095-370

P-72

FINAL REPORT

SYNTHESIS OF INDIVIDUAL ROTOR BLADE CONTROL SYSTEM FOR GUST ALLEVIATION

By Ji C. Wang

Alphonse Y. Chu

Mechanical Engineering Department
San Jose State University
San Jose,CA 95192

Peter D. Talbot

Rotorcraft Technology Branch
NASA Ames Research Center

Prepared For : National Aeronautics and Space Administration
Rotorcraft Technology Branch
Ames Research Center
Moffett Field, CA
Under Contract NCC 2-267

July, 1990

ACKNOWLEDGEMENTS

This report documents a research conducted by San Jose State University for NASA Ames Research Center under Contract No. NCC 2-267.

This contract was administered by the Rotorcraft Technology Branch of NASA Ames. Mr. Peter D. Talbot was the NASA collaborator and was the NASA's technical monitor.

TABLES OF CONTENTS

LIST OF FIGURES

CHAPTER 1

INTRODUCTION

In the early days of helicopter development, the blades were rigidly attached to the rotor hub. It was observed by pioneers like Sikorsky and Juan de la Cierva that their helicopters, which were called autogyros, could hover and climb vertically. Yet the machine failed to fly forward, and in fact it would get out of control and rolled over. Cierva was especially puzzled by this phenomenon since he was able to fly a model built with flexible spars without problem[1].

It was later discovered that the way the rotor blades were attached to the shaft hub was responsible for the control problem with the autogyro. Cierva's full-scale prototype had the rotor rigidly connected to the shaft with wires while the model was made of flexible material. Figure 1.1 illustrates the velocity distribution of a helicopter rotor blade in forward flight. During hover, air speed encountered by each blade is the same. As the helicopter flies forward, the air speed experienced by an individual blade varies depending on the azimuth angle and radial position during each revolution. On the advancing side, the resultant speed is higher than the retreating side. There is a region of reverse flow on the retreating side where the forward speed exceeds the speed due to blade rotation.

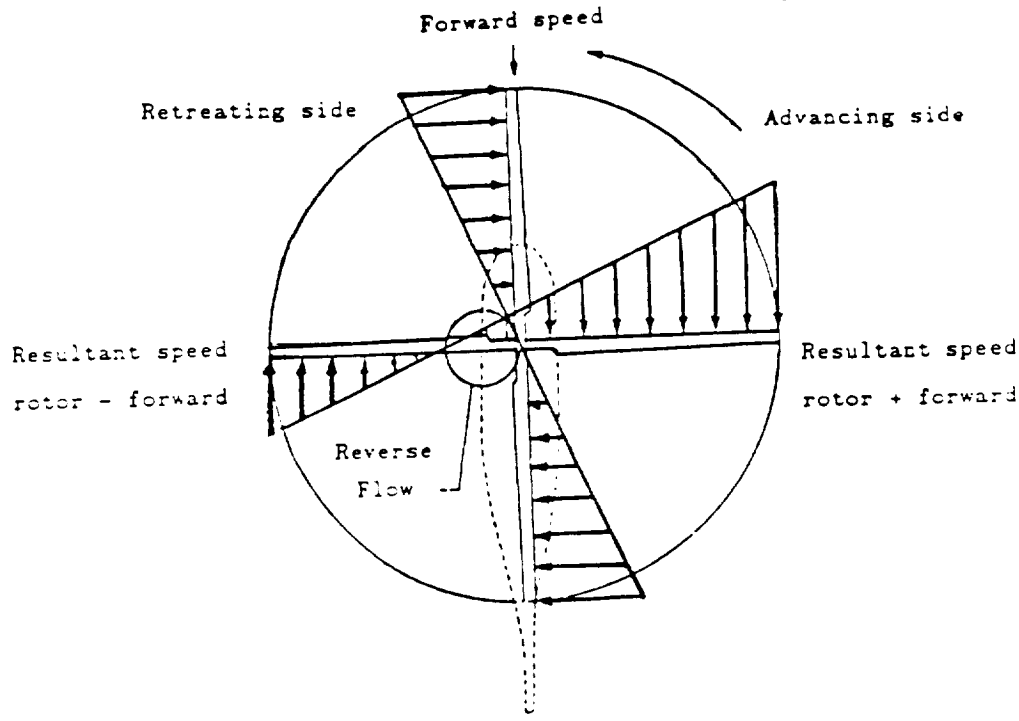

Figure 1.1 Velocity Distribution during Forward Flight

When stiffly attached to the shaft, such as the case of Cierva's autogyro, each blade had the same pitch setting, thus angle of attack. As the resultant velocity was higher on the advancing side, more lift was generated. The difference in lift between the two sides resulted in a rolling couple. Since this was not compensated for, the helicopter toppled. On the other hand, if the blades were allowed to move up and down freely, the ones on the advancing side would begin to flap upward because of higher lift. As it flapped up, the angle of attack was decreased, resulting in lower lift. Maximum flapping for a blade hinged

at the center of the shaft occurred at the nose of the helicopter. Meanwhile, experiencing lower lift, the retreating blade started to descend as it rotated towards the tail. Its angle of attack was decreased until the retreating blade reached the position over the tail, where the local velocity attained a mean value. When the blades were allowed to flap up and down, the rotor maintained a fore and aft tilt position such that the lift distribution was balanced and the machine remained stable.

Flapping is a phenomenon arisen from the need to balance the moment produced by aerodynamic, inertial and centrifugal forces about the Center of Gravity. The front and back, or longitudinal, flapping discussed above is caused by asymmetric velocity distribution during forward flight. Besides longitudinal flapping, a rotor blade also flaps laterally due to coning. In order for the rotor blade to achieve an equilibrium position during flapping, its angle of attack has to be just sufficient to compensate for the speed at each point during a revolution. The amount of flapping also depends on the stiffness of the rotor. In flight, a rotor with flapping hinges will maintain a slightly coned shape with the lift providing the upward force and the centrifugal force keeping the blades extended.

The idea of having hinge in a blade was further utilized in the rotor technology. By incorporating a second hinge in the plane of the rotor disk, the blade can move

freely without causing stress in the rotor root. This hinge is known as lead-lag hinge and together with flapping hinge, result in the fully articulated rotor used extensively nowadays.

The ability for a helicopter rotor to flap is an important factor in both stability and control. The attitude of the tip-path-plane determines the thrust vector in space. To control a modern helicopter, the pilot changes the pitch of the blade cyclically about the feathering axes by tilting the swash plate. The angle between the rotor shaft and the tip-path-plane is defined as the flapping angle while the angle between the shaft and the swash plate is called feathering angle. In forward flight at constant speed, the orientation of tip-path-plane is fixed in space. This can be achieved with more than one trim condition. One of such conditions has the tip-path-plane perpendicular to the rotor shaft. Flapping angle is, by definition, zero and only feathering is used to maintain the thrust vector. On the other hand, a different center of gravity position or horizontal stabilizer setting can result in the same trim condition with the swash plate being perpendicular to the shaft. In this case, there is no feathering and flapping is the sole means of control. Typically, both flapping and feathering are used to realize the required tip-path-plane orientation.

Flapping can be introduced by either the pilot as a

mechanism of controlling a helicopter, or by gust disturbance. Gust is undesirable because it has deteriorating effects on the handling qualities of a helicopter. Handling qualities is perceived by pilot in terms of both stability and control. The ability of the pilot to hold the attitude in the presence of gust is a stability characteristic. Conversely, if it takes a lot of efforts for him to change the altitude of the helicopter under windy conditions, the pilot will view the control as sluggish. Therefore, it is critical to minimize the flapping caused by gust.

Norman Ham of MIT has been working on the idea of IBC (Individual Blade Control)[2]. The method employs blade mounted sensors to measure the flapping motion parameters and applies the processed information to control the root pitch of each individual blade. As a result, flapping caused by gust disturbance is reduced. The net effect is a tighter control over the tip-path-plane, resulting in improvement of the vehicle's handling qualities.

This thesis attempts to demonstrate the utilization of rotor flapping in synthesizing an IBC system for gust alleviation. The objective of this study is to illustrate and seek to improve Ham's IBC method. A sensor arrangement with two accelerometers mounted on the root and tip of a blade is proposed for estimating of flapping states for feedback control. Equivalent swash plate implementation of

IBC is also deliberated. The study concludes by addressing the concept of general rotor states feedback, of which the IBC method is a special case.

This thesis is consisted of eight chapters. The following is a brief summary of each chapter. The blade flapping equation of motion is derived in Chapter 2. Ham's original IBC method and a modified IBC scheme called Model Reference (MRIBC) are examined in Chapter 3, followed by simulation study with ideal measurements and relative performances of the two methods in Chapter 4. The practical aspects of IBC implementation are presented in Chapter 5. Different configuration of sensors and their merits are considered. In Chapter 6, the realization of IBC using equivalent swash plate instead of direct actuator motion is discussed. It is shown in Chapter 7 that IBC is a particular case of rotor states feedback. The idea of general rotor states feedback is further elaborated here. Finally, major conclusions of this thesis are given in Chapter 8.

CHAPTER 2

BLADE FLAPPING EQUATION OF MOTION

The equation governing the rigid flapping motion β of a single articulated blade in a rotating coordinate system may be approximated by a linear differential equation [3,4]:

$$\ddot{\beta} + A(\mu,\phi)\dot{\beta} + B(\mu,\phi)\beta = C(\mu,\phi)\theta + W_g(\mu,w,\Omega) \qquad (1)$$

where

β = blade flapping angle

μ = advance ratio

ϕ = blade azimuth angle

θ = collective and cyclic pitch control input

W_g = Disturbance gust input

w = frequency of gust

Ω = rotor speed

The coefficients in the equation of motion are periodic in ϕ, and are function of μ. The equation is reduced to a ordinary linear differential equation with constant coefficients in hover, when $\mu = 0$.

The equation of motion can be derived by summing moments about the articulated offset hinge, as shown in Figure 2.1. Forces acting on an element of mass dm are : 1) aerodynamic lift force dL, 2) force due to tangential acceleration of flapping $(r-e)\ddot{\beta}$ x dm and 3) centrifugal force due to rotation about the rotor shaft $r\Omega^2$ x dm.

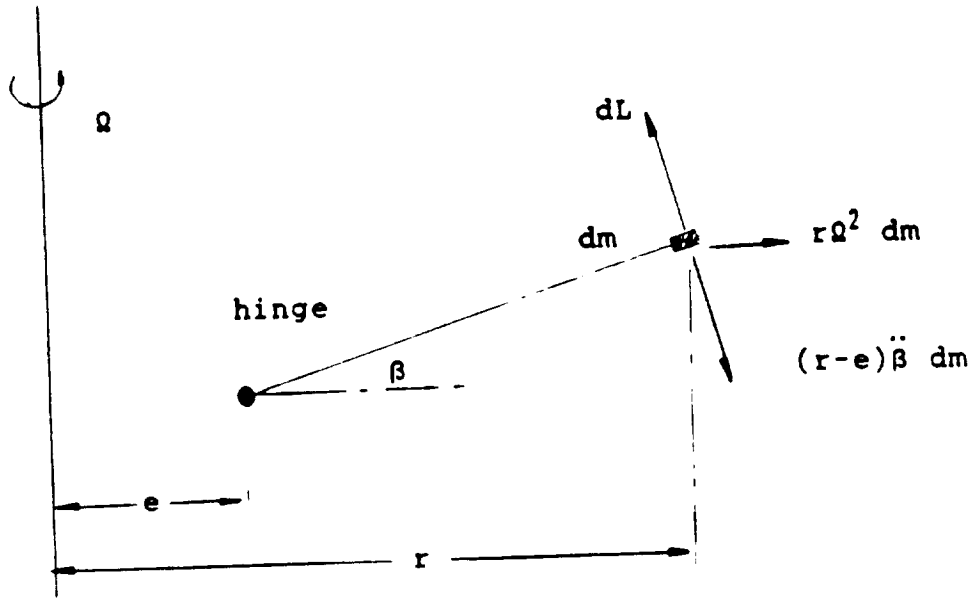

Figure 2.1 Forces acting on a blade element

By using harmonic balance technique[5], the pitch and gust inputs can be expressed in assumed harmonic motion forms. The root pitch input θ assumes a harmonic motion of steady-state term plus harmonics at rotor rotation frequency Ω :

$$\theta = \theta_0 - A_{1s} \cos\Omega t - B_{1s} \sin\Omega t \qquad (2)$$

The gust input assumes the form of a sine wave of frequency w and first subharmonic (Ω - w) and superharmonic (Ω + w) of the rotation frequency :

$$W_g = a_1 \sin wt + b_1 (\cos(\Omega - w)t - \cos(\Omega + w)t) * \mu \qquad (3)$$

Assumptions made in deriving the above blade flapping equation of motion are :

1) The blade is rigid.
2) Only a single blade is considered, there is no interaction with the fuselage.
3) Flapping is assumed to take place in the pitch plane, there is no coupling with the roll or yaw axis.
4) In deriving the equation, any higher order terms beyond second of the normalized flapping hinge offset ϵ are dropped.
5) The inflow of air to the rotor disc due to forward flight is lumped into the gust term W_g.
6) The rotor speed is constant.
7) Gravitational force on the blade is neglected; only inertial and aerodynamic forces are being considered.

CHAPTER 3

IBC ANALYTICAL FEEDBACK CONTROL

A helicopter, compared to an airplane of similar size, provides a smoother ride in the presence of gust. Since the rotor blades flap individually to reduce the pitch and roll rate, the fuselage and the rest of the helicopter are shielded from the disturbance. In contrast, the wings of an airplane simply transmit the wing loads, either as disturbance or lift, to the fuselage. The result is a rougher ride.

The air space around a helicopter rotor is a very complex aerodynamic environment. The frequency response of a blade can be divided into two categories according to the frequency contents of the excitation. The first one is the low frequency range from 0 to 1 Ω (rotational speed), which includes gust response, blade instability due to flap-lag coupling, and ground resonance. The second category is a high frequency domain above 1 Ω involving blade bending stress, vibration, noise and higher harmonic motion. The blade flapping mode, which completes a cycle during one blade revolution, has a natural frequency of approximately 1 Ω. This mode dominates low frequency effects such as gust response and flying qualities. Since blade flapping is a means by which the pilot trims and controls the helicopter, any unwanted blade flapping due to gust is viewed as an external disturbance to be attenuated.

Methods of IBC Analysis

To best illustrate IBC technique, general methods used to analyze systems described by differential equation with periodic coefficients will be discussed, followed by the particular IBC control algorithm used by Ham. Finally, a modified approach termed MRIBC (Model Reference Individual Blade Control), is presented for possible improvement of the IBC concept. The equation describing the rigid flapping motion of a single articulated blade in a rotating coordinate system can be approximated by a linear differential equation with periodic coefficients :

$$\ddot{\beta} + A(\mu,\phi)\dot{\beta} + B(\mu,\phi)\beta = C(\mu,\phi)\theta + W_g(\mu,w,\Omega) \qquad (1)$$

Many features of analysis and synthesis of linear time-invariant system, such as eigenvalues and linear quadratic synthesis, can be applied to a linear periodic system, according to Floquet theory[4,6]. The theory states that if the solution of a linear periodic system is sampled at intervals of one system period, the sampled solution behaves as a time-invariant system. As the first step in designing a controller for the IBC system, the periodic system is transformed into a time-invariant one. Linear quadratic synthesis can then be employed to determine a set of control gains which optimizes a particular cost function.

Ham's IBC (Individual Blade Control)

Norman Ham of MIT has been doing research work on IBC concept. IBC is an active control in which each blade is separately controlled in the rotating frame by attaching broad-bang electrohydraulic actuators to the swash plate or individually to each blade. The control signal is generated from sensors mounted on the blades. IBC involves not just control of each blade independently, it also provides a feedback loop for each blade in the rotating frame.

In Ham's IBC design, the controller design (blade flapping angle, angular rate and angular acceleration feedback gains) was not conducted using multi-variable states feedback control methods such as linear quadratic analysis. Instead, the feedback gains were selected such that the closed-loop blade dynamic behavior was the same as the open loop's, with the exception of a reduced gust term. The derivation of Ham's IBC scheme is given in Appendix A. In Chapter 6, it is shown that Ham's IBC scheme is a limited case of multi-variable rotor states feedback control system. Figure 3.1 shows a block diagram of the open loop system. θ_{swp} is the trimmed collective and cyclic pitch input from the swash plate to sustain the forward flight. W_g is the disturbance gust input. A typical plot of input and output for this open loop system is depicted in Figure 3.2. When the output angle, rate and acceleration are fed back, as

illustrated in Figure 3.3, a full state feed back IBC system is formed.

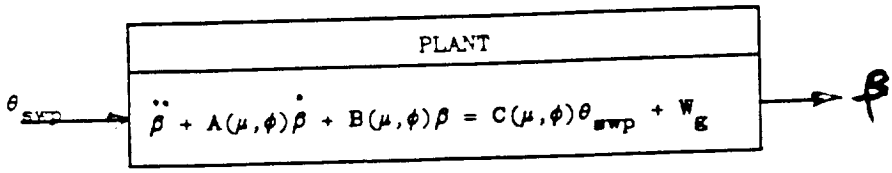

Figure 3.1 Open loop flapping equation

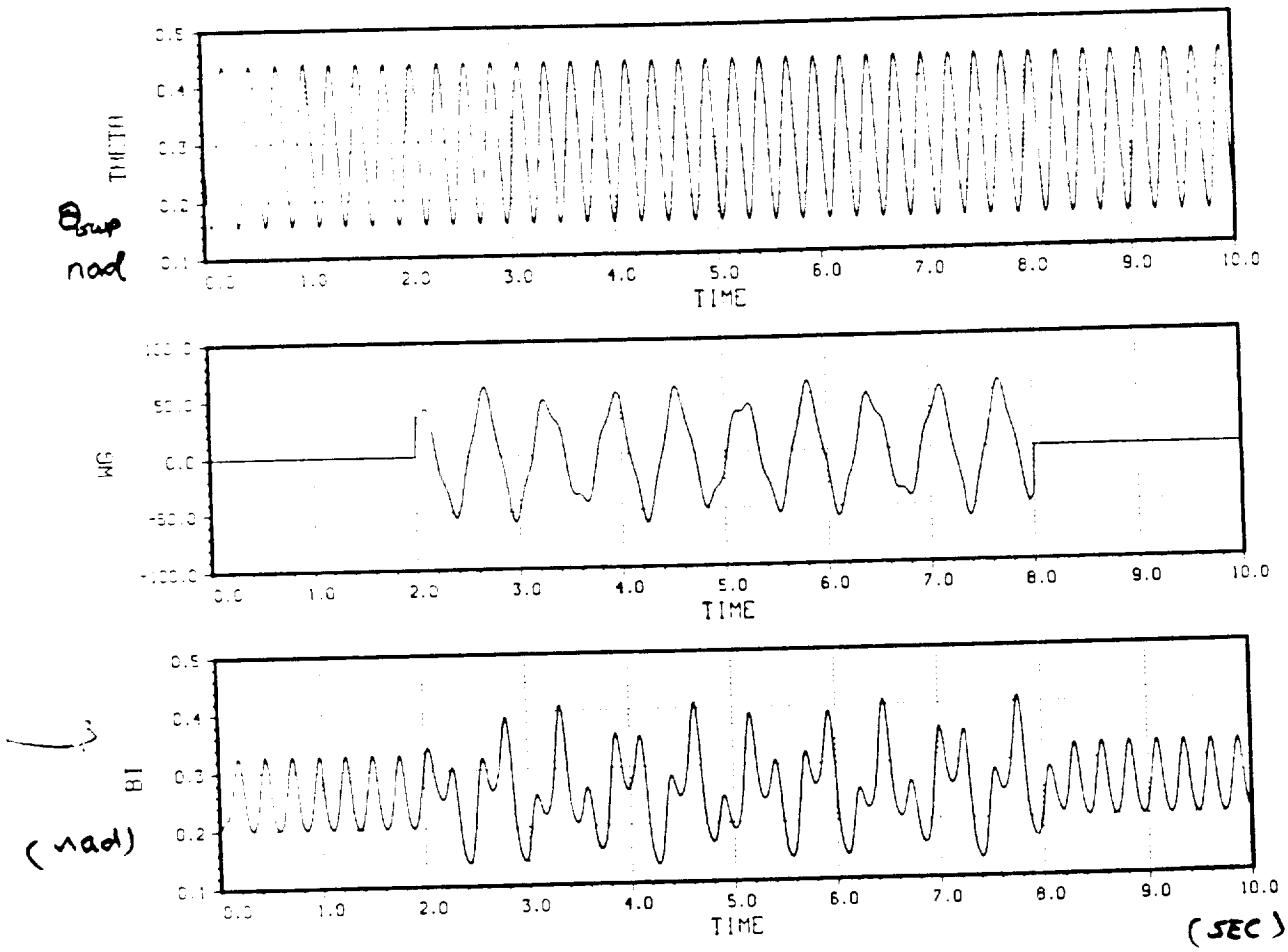

Figure 3.2 Open loop response

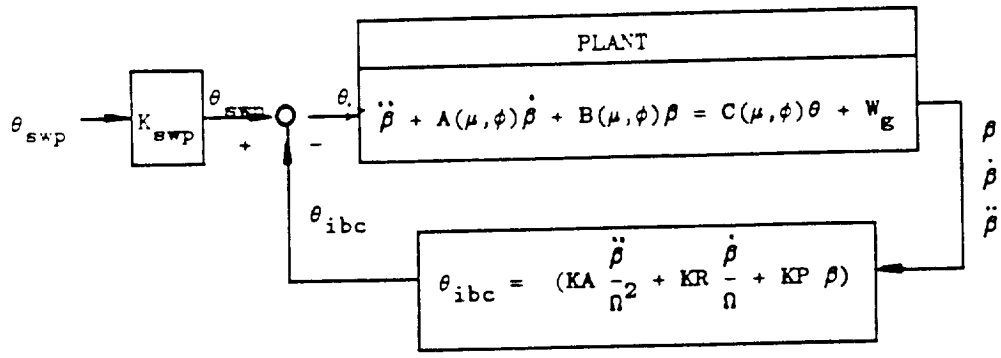

Figure 3.3 Ham's IBC method

Periodic controller gains are difficult to implement physically. It also places a lot of demands on the actuator. A set of constant gains may be chosen for feedback while the flapping equation of motion still maintains the same periodic coefficients. This configuration is being investigated as an alternative to the time-varying gain model in a simulation study in Chapter 4.

Another viable approach to Ham's IBC is apparent when a closer look is taken at the equation of motion. The periodic coefficients are cosine and sine functions multiplied by first and second order terms in μ. These terms will not vary much when μ is close to zero. A constant coefficient model of the blade flapping equation may be valid for low advance ratio. In reference 2, a Floquet analysis was performed to the flapping equation of motion and it was found that the

eigenvalues of the blade characteristic equation did not vary significantly for $\mu < 0.3$.

Model Reference IBC

It is desirable to have a control law which is less sensitive to the DC value of the control input. Too high a DC value has degrading effects on the handling qualities of a helicopter. A Model Reference IBC system is proposed. A block diagram of the system is shown in Figure 3.4.

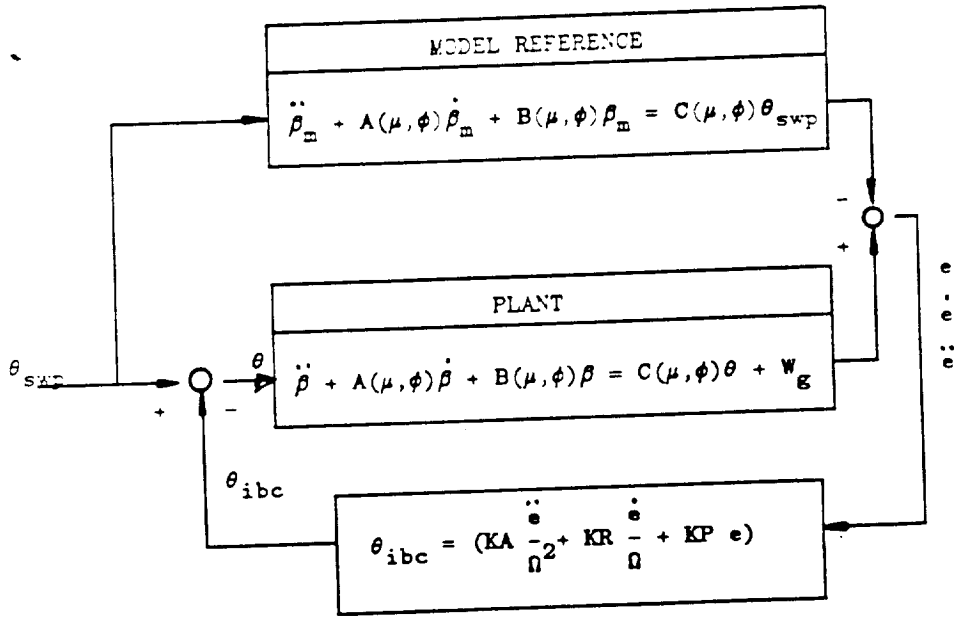

Figure 3.4 Model Reference IBC method

A math model of the plant can be built using technique such as parameter identification. The differences between the plant and the model states, rather than the plant states themselves, are used to formulate the feedback control law. The IBC control is a function of the error signal e, and therefore less sensitive to DC value of the control input. Derivation of the equations for MRIBC method is shown in Appendix B.

Owing to the scope of the present studies, some essential subsystems in IBC are not addressed. For instance, the actuator dynamics is ignored in the analyses. Actuator is basically a low-pass servo system. When it is placed in the feedback loop in Figure 3.3, θ_{ibc} will contain only the low frequency portion of the original signal. High frequency flapping disturbance will not be affected by the IBC system since the high frequency content of the feedback signal is filtered. Flapping states β, $\dot{\beta}$, $\ddot{\beta}$, used in determining θ_{ibc} are either measured or estimated. In both cases, the signal is corrupted due to presence of noise. Low pass filters are usually required before this signal can be utilized. This will introduce delay (phase shift) in addition to effects on the overall stability of the whole IBC system.

CHAPTER 4

SIMULATION ANALYSIS OF IBC WITH IDEAL MEASUREMENTS

A simulation study was performed to evaluate the IBC schemes employing the Model Reference method and the original one conceived by Ham. The simulation runs were made using a VAX digital computer. A fourth order Runge-Kutta method was utilized for numerically solving the differential equations of motion. Integration step size was 0.001 second. A generic UH-60 Black Hawk rotor blade was chosen for the study. Effects due to fuselage interaction or actuator was not considered. In the simulation, sensor dynamics was ignored and perfect measurements of flapping angle, rate and acceleration were presumed available.

Ham's IBC Method

Three approaches were made in analyzing Ham's IBC method. The first approach employed the full periodic flapping equation of motion with time-varying feedback control gains. The second method still used periodic coefficients for the equation. The controller gains were, however, independent of time. They were computed as average value of the time-varying gains. In the third approach, constant coefficients were assumed for the flapping motion, resulting in constant gains. It is known as simplified Ham's IBC method in this study.

To investigate the effects of IBC on gust alleviation,

both the open and closed loop flapping angles were plotted on the same graph. Peak to peak values of the two angle responses were measured and the percentage of reduction due to feedback computed. For example, Figure 4.1 shows, for the first approach of periodic coefficients and gains, the decrease in flapping angle response when the gain KA takes on a value of .35 and 1.2. The dotted curve is open loop response (KA = 0) and the solid one represents the response when IBC is in effect.

In Ham's second IBC approach, an effort was made to find a set of constant feedback gains which would work reasonably well for the time-varying flapping equation of motion. It was observed that the system became unstable when the gain KA was over 0.55. The results are summarized in Figure 4.2 for KA = 0.35 and 0.575. There appears to be a phase swift in the angle response between the open loop (KA = 0) and KA ≠ 0 case. This method is not further pursued in the current study.

Discussion of Results

Sensitivities of flapping angle response to control gains are demonstrated in Figures 4.3 and 4.4 for first and third approach respectively. Gust effect is seen to be reduced by increasing the value of KA. For any given value of KA, the first approach with time-varying gains tends to achieve a better performance in reducing flapping due to

gust disturbance. On the other hand, the simplified IBC is easier to implement since a constant set of feedback gains is used through out the flight.

As shown in Figures 4.5 and 4.6, the magnitude of the IBC control input, θ_{ibc}, also gets larger with increasing KA. Furthermore, even though the magnitude of the total control input TTOL, defined as the sum of IBC control and swash plate input, remains about the same, its DC value increases as KA is changed from 0.35 to 1.2. This increase in DC value is equivalent to adding an extra collective pitch input due to swash plate motion. An excessive DC value may impair the vehicle's flight qualities. The allowable peak to peak value of the control input places an upper limit on KA. A realistic upper bound of KA is about 1.2.

From the derivation in Appendix A, it is established that, in theory, the gust term can be reduced by a factor of $1/K_g$ using Ham's IBC method. For the simplified IBC scheme with constant coefficients and gains, $K_g = 1 + KA$. Thus, a theoretical reduction of 50% in gust input can be accomplished with KA = 1 for the simplified IBC method. The corresponding reduction in flapping response β is not necessarily the same in magnitude. The simulation results in Figure 4.8 show that a reduction of 20% in flapping response is achieved when KA = 1.

MRIBC (Model Reference IBC) Method

In this study, the plant was modelled by differential equation with time-varying coefficients. Two model reference control schemes, one with time-varying math model and feedback gains and the other with time-invariant model and gains were simulated.

Discussion of Results

A typical time history of θ_{ibc} and β for MRIBC with time-varying math model is shown in Figure 4.7. Note that the feedback signal θ_{ibc} has a DC value of zero. This is a characteristic of MRIBC since θ_{ibc} depends only on the differences in the plant and model states. MRIBC control activity is minimum with absence of gust disturbance on the blade. Between the methods with constant math model and time-varying model, the latter exhibits higher percentage of gust reduction for the same KA. The results are summarized in Figures 4.8 and 4.9. As KA is increased, both models become unstable eventually. This happens at KA > 0.75 for the time-varying math model. The model with constant coefficients will be unstable if KA > 1.2.

MRIBC with time-varying math model of the plant shows performance comparable to that of the original IBC's. In fact, for KA = 0.5, MRIBC has a slight edge over IBC. However, MRIBC becomes unstable rather quickly. MRIBC with time-invariant math model generally has smaller percentage of gust reduction than simplified IBC.

As previously discussed, MRIBC has an control input whose DC value is less sensitive to variation of controller gain KA than IBC. This property is illustrated in Figures 4.10 and 4.11. While Ham's simplified IBC is shown in Figure 4.11 to have a θ_{ibc} with DC value of about -0.2 rad., the corresponding value is essentially zero in the case of MRIBC with time-invariant math model.

CHAPTER 5

ESTIMATION OF BLADE STATE VARIABLES

For any of the above IBC schemes to work, blade angular displacement, angular rate and angular acceleration are needed to generate the feedback signal. The information can definitely be obtained by direct sensor measurements, as in the case of full blade state variables feedback. However, there are several disadvantages with measuring all states directly. First of all, sensors are expensive and they add complexity to the overall system. Secondly, there is always noise associated with any measurement. In certain cases, the noise present may make an otherwise stable system unstable. To counteract the noise, filters are invariably required for these sensor data, again adding cost and complexity.

Figure 5.1 shows a block diagram of a typical closed-loop estimator.

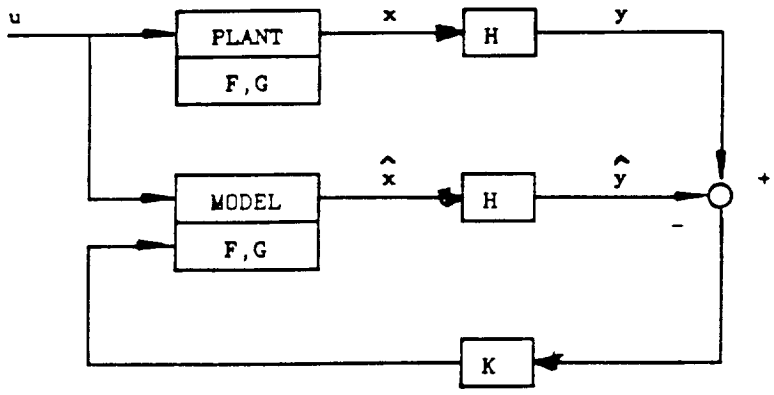

Figure 5.1 Closed-loop estimator

The idea of estimator is to make use of algorithm to reconstruct all the blade states given only measurement of some of them. A plant is represented by a set of first order differential equations :

$$\dot{X} = F X + G U \tag{1}$$

Let $\hat{X}$ = estimate of X

$$\dot{\hat{X}} = F \hat{X} + G U + K(Y - \hat{Y}) \tag{2}$$

$$= F \hat{X} + G U + K(Y - H \hat{X})$$

Let $\tilde{X}$ = estimation error = $X - \hat{X}$

$$\dot{\tilde{X}} = \dot{X} - \dot{\hat{X}}$$

$$= FX + GU - [F\hat{X} - GU + K(Y - H\hat{X})]$$

$$= (F - K H) \tilde{X}$$

This is a homogeneous differential equation. Values of the estimator feedback gain vector K can be chosen such that the estimator system matrix (F - K H) represents a stable system. Furthermore, K should be selected such that the estimator system, and therefore the estimation error, converges to zero as fast as possible. When this happens, $\hat{X}$ will converge to X regardless of the value of $\hat{X}(0)$. For the selection of the gain vector K, the characteristic equation of the system matrix (F - K H) is computed. The coefficients of like powers of this equation are then compared to the equation formed with the desired estimator root locations in

the s-plane. K is uniquely determined if the output variable y is a scalar, i.e. there is only one non-zero element in the row matrix H.

Estimator roots are picked to be faster than those of the plant so that total response is dominated by the response due to the plant. The faster the estimator roots, the quicker the error converges. Upper limit to the estimator response speed depends on noise rejection characteristics and sensitivity to model errors. In the simulation, the estimator roots were selected at least 4 times faster than the plant's. In the following section, the performances of two estimators, namely Direct Flap Estimator and IBC Kinematic Estimator are evaluated.

Direct Flap Estimator

Direct flap estimator uses only the flapping angle β to estimate β, $\dot{\beta}$ and $\ddot{\beta}$. In state space form, the open loop flapping equation of motion is written in the form of (1) as:

$$F = \begin{bmatrix} 0 & I \\ -B & -A \end{bmatrix} \quad ; \quad X = \begin{bmatrix} \beta \\ \dot{\beta} \end{bmatrix}$$

$$U = \theta_{swp} + W_g$$

$$G = [0, \quad 1]^T$$

$$H = [1, \quad 0]$$

In state space form, the estimator for the blade flapping equation of motion is given as :

$$\frac{d}{dt}\begin{bmatrix}\hat{\beta}\\ \dot{\hat{\beta}}\end{bmatrix} = \begin{bmatrix}0 & I\\ -B & -A\end{bmatrix}\begin{bmatrix}\hat{\beta}\\ \dot{\hat{\beta}}\end{bmatrix} + \begin{bmatrix}0\\ \theta_{swp}+W_g\end{bmatrix} + \begin{bmatrix}K_1\\ K_2\end{bmatrix}\ [\beta - \hat{\beta}] \qquad (3)$$

Case 1-A, Direct Flap Estimator

The coefficients A, B are being utilized as feedforward terms and the estimation error $[\beta - \hat{\beta}]$ as feedback term. Ham's simplified model with constant coefficients and controller gains was employed to demonstrate the performance of the estimator. The estimator roots were set about 4 times faster than the fastest plant root. The result is shown in Figure 5.2. The dotted and the solid lines represent the true and estimated states respectively. The estimated angle follows the true one very closely and the rate is doing reasonably well.

Case 1-B, Direct Flap Estimator

The plant dynamics change with flight conditions, and is therefore time-varying. The flapping equation is a function of forward air speed and blade azimuth angle. If the estimator roots are to be maintained throughout the flight, estimator gains will have to be adjusted continuously[6]. This can be done by gain scheduling as a

function of flight conditions. However, this is not an easy task as the combinations of flight conditions are numerous. If the plant dynamics are taken out by setting A, B and the input matrix to zero, a set of constant estimator gains can be utilized through out the flight. The model becomes known as kinematic estimator[7,8]. The equation below describes such an estimator.

$$\frac{d}{dt}\begin{bmatrix}\hat{\beta}\\ \dot{\hat{\beta}}\end{bmatrix} = \begin{bmatrix}0 & I\\ 0 & 0\end{bmatrix}\begin{bmatrix}\hat{\beta}\\ \dot{\hat{\beta}}\end{bmatrix} + \begin{bmatrix}K_1\\ K_2\end{bmatrix}[\beta - \hat{\beta}] \qquad (4)$$

By analogy with classical control theory, Equation (4) characterizes PI (proportional plus integral) control since the estimation error is used to update both the angle and the rate. The effectiveness of the kinematic estimator is depicted in Figure 5.3. It does not track the plant as well as the previous estimator in Equation (3) which includes the plant dynamics.

The kinematic estimator described by Equation (4) employs β to estimate both β and $\dot{\beta}$. Since acceleration $\ddot{\beta}$ is also needed for the IBC schemes, the estimator in Equation (4) will be extended to provide $\ddot{\beta}$ information. Two cases are considered. The first one is essentially two Direct Flap Case 1-B estimators cascaded together. Figure 5.4 illustrates this method. The output of the first estimation,

$\hat{\dot{\beta}}$ is used as input to predict $\hat{\ddot{\beta}}$. It is seen from Figure 5.5 that while the angle can be tracked very well, the estimated acceleration lags behind the true one. The second case is delineated by Equation 5.5.

$$\frac{d}{dt}\begin{bmatrix}\hat{\beta}\\ \hat{\dot{\beta}}\\ \hat{\ddot{\beta}}\end{bmatrix} = \begin{bmatrix}0 & I & 0\\ 0 & 0 & I\\ 0 & 0 & 0\end{bmatrix}\begin{bmatrix}\hat{\beta}\\ \hat{\dot{\beta}}\\ \hat{\ddot{\beta}}\end{bmatrix} + \begin{bmatrix}K_1\\ K_2\\ K_3\end{bmatrix}[\beta - \hat{\beta}] \qquad (5)$$

The system matrix is 3 x 3. Three estimator roots close to the ones used in equation (4) were chosen to evaluate this implementation. The performance is similar to case one above, as shown in Figure 5.6.

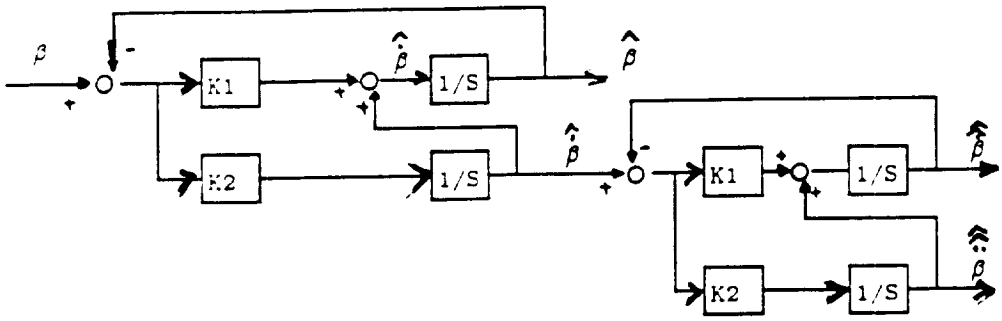

Figure 5.4 Cascaded Direct Flap estimator

IBC Kinematic Estimator

For the Direct Flap estimators described above, measurement of flapping angle is required to estimate β, $\dot{\beta}$ and $\ddot{\beta}$. This can be done by attaching a strain gauge at the

blade root fitting. A better technique to deduce all three states needed for IBC is to use two accelerometers mounted at the root and tip of a blade[7]. In this IBC Kinematic Estimator method, the two accelerometers provide both β and $\ddot{\beta}$ information, from which $\dot{\beta}$ can also be estimated. A block diagram for this approach is given in Figure 5.7.

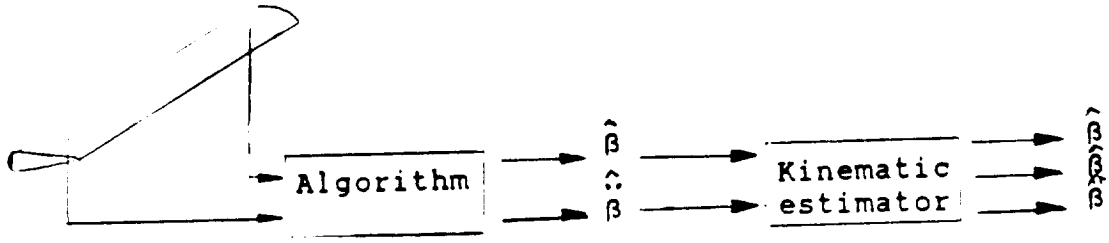

Figure 5.7 IBC Kinematic Estimator block diagram

An accelerometer positioned along an hinged blade experiences inertial force as shown in Figure 5.8.

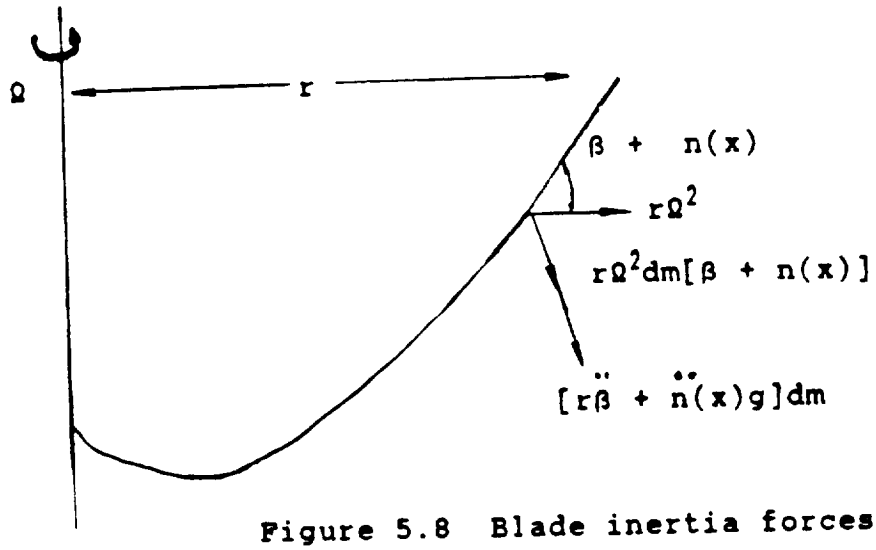

Figure 5.8 Blade inertia forces

The signal $a_f(x)$ is in response to both the flapping and first elastic flatwise bending mode.

$a_f(x)$ is given by [2]:

$$a_f(x) = R\Omega^2 \left(x\ddot{\beta}/\Omega^2 + x\beta + \ddot{n}(x)g/\Omega^2 + xn(x)g \right) \qquad (6)$$

where R = rotor radius

Ω = rotor speed

x = blade spanwise location $(x - e)/R$

β = blade flapping angle

$n(x)$ = first elastic flatwise bending mode shape

g = first elastic flatwise bending mode displacement

The first elastic bending mode has a natural frequency at about 2 Ω. If a low pass filter with bandwidth up to 1 Ω is used, the flapping mode, which has a natural frequency between 0 and 1 Ω, will be preserved while the first elastic bending mode is attenuated. With such a low pass filter, the accelerometer signal becomes :

$$a_f(x) = R\Omega^2 \left(x\ddot{\beta}/\Omega^2 + x\beta \right) \qquad (7)$$

This is an algebra equation with two unknowns on the

right hand side. With two accelerometers placed at different locations on the blade, two such equations are obtained. Both flapping angle and acceleration can then be solved for. Written in scalar form, Equation (4) becomes :

$$\frac{d\hat{\beta}}{dt} = \hat{\dot{\beta}} + K_1 \ (\beta - \hat{\beta})$$

$$\frac{d\hat{\dot{\beta}}}{dt} = \qquad K_2 \ (\beta - \hat{\beta}) \qquad (8)$$

Equation (8) is modified to accommodate the additional flapping acceleration information. The IBC Kinematic Estimator equation can be expressed as :

$$\frac{d\hat{\beta}}{dt} = \hat{\dot{\beta}} + K_1 \ (\beta - \hat{\beta})$$

$$\frac{d\hat{\dot{\beta}}}{dt} = \ddot{\beta} + K_2 \ (\beta - \hat{\beta}) \qquad (9)$$

Since both β and $\ddot{\beta}$ are available, the task of estimating $\dot{\beta}$ is not difficult. In fact, the estimated $\hat{\dot{\beta}}$ tracks the true one very closely after a transient duration of 0.5 second.

CHAPTER 6

IMPLEMENTATION OF IBC THROUGH SWASH PLATE ACTUATORS

All the IBC methods discussed so far utilize an individual actuator to change the pitch of each blade. This is direct control in the rotating frame. IBC is executed using these actuators, which rotate with the blade while pilot control is achieved using a conventional swash plate in non-rotating frame. In this configuration, actuator reliability is always a concern, and it may be more significant than the simplicity such a system offers. As an alternative, by attaching actuators to the swash plate, the same degrees of individual blade control can be accomplished in a pure non-rotating frame.

A helicopter with swash plate has three control degrees-of-freedom : collective, longitudinal and lateral cyclic. For a helicopter with three blades, the number of control degrees-of-freedom is equal to the number of blades. When four blades are present, as in the case of Black Hawk, an equivalent swash plate implementation of IBC can also be formulated. For a four bladed helicopter, a transformation between the rotating coordinate system and the non-rotating system is given as :

$$\Delta \underline{\theta}_{ibc} = TR \, \Delta \underline{\theta}_{swp}$$

where $\Delta \underline{\theta}_{ibc} = [\, \Delta\theta_1, \Delta\theta_2, \Delta\theta_3, \Delta\theta_4 \,]^T$ is the individual blade pitch control angle vector in the rotating reference frame,

and $\Delta \underline{\theta}_{swp} = [\, \Delta\theta_{cl}, \Delta A_{1s}, \Delta B_{1s}, \Delta\theta_{\frac{1}{2}} \,]^T$ is the ideal swash plate displacement vector in the non-rotating frame. $\Delta\theta_i$ is any element of $\Delta \underline{\theta}_{ibc}$. It can be expressed in elements of swash plate displacement vector as

$$\Delta\theta_i = \Delta\theta_{cl} + \Delta A_{1s} \cos\phi_i + \Delta B_{1s} \sin\phi_i + \Delta\theta_{\frac{1}{2}} (-1)^i \qquad (1)$$

for i = 1,2,3,4 in the case of a four-blade system. Thus, the transformation matrix can be expressed as

$$TR = \begin{bmatrix} 1 & C\phi_1 & S\phi_1 & -1 \\ 1 & -S\phi_1 & C\phi_1 & 1 \\ 1 & -C\phi_1 & -S\phi_1 & -1 \\ 1 & S\phi_1 & -C\phi_1 & 1 \end{bmatrix} \qquad (2)$$

where ϕ = azimuth angle, $C\phi_1 = \cos\phi_1$, $S\phi_1 = \sin\phi_1$

An equivalent swash plate motion for a given $\underline{\theta}_{ibc}$ can be derived as

$$\Delta \underline{\theta}_{swp} = TR^{-1} \Delta \underline{\theta}_{ibc}$$

where

$$TR^{-1} = 1/2 \begin{bmatrix} 1/2 & 1/2 & 1/2 & 1/2 \\ C\phi_1 & -S\phi_1 & -C\phi_1 & S\phi_1 \\ S\phi_1 & C\phi_1 & -S\phi_1 & -C\phi_1 \\ 1/2 & 1/2 & 1/2 & 1/2 \end{bmatrix} \qquad (3)$$

Since the current swash plate mechanism has only three control degrees of freedom, $\Delta\theta_{\frac{1}{2}}$ does not exist. Only $[\, \Delta\theta_{cl}, \Delta A_{1s}, \Delta B_{1s} \,]$ motion can be realized in real application. If they are fed back to the rotor system, then

$$\begin{bmatrix} \theta_{cl} \\ A_{1s} \\ B_{1s} \end{bmatrix} = 1/2 \begin{bmatrix} 1/2 & 1/2 & 1/2 & 1/2 \\ C\phi_1 & -S\phi_1 & -C\phi_1 & S\phi_1 \\ S\phi_1 & C\phi_1 & -S\phi_1 & -C\phi_1 \end{bmatrix} \begin{bmatrix} \theta_1 \\ \theta_2 \\ \theta_3 \\ \theta_4 \end{bmatrix} \quad (4)$$

The equivalent blade pitch angle becomes

$$\begin{bmatrix} \theta_1 \\ \theta_2 \\ \theta_3 \\ \theta_4 \end{bmatrix} = \begin{bmatrix} 1 & C\phi_1 & S\phi_1 & -1 \\ 1 & -S\phi_1 & C\phi_1 & 1 \\ 1 & -C\phi_1 & -S\phi_1 & -1 \\ 1 & S\phi_1 & -C\phi_1 & 1 \end{bmatrix} \begin{bmatrix} \theta_{cl} \\ A_{1s} \\ B_{1s} \end{bmatrix} \quad (5)$$

When Equation (4) is substituted into (5)

$$\begin{bmatrix} \theta_1 \\ \theta_2 \\ \theta_3 \\ \theta_4 \end{bmatrix} = \begin{bmatrix} 3/4 & 3/4 & -1/4 & 1/4 \\ 1/4 & 3/4 & 1/4 & -1/4 \\ -1/4 & 1/4 & 3/4 & 1/4 \\ 1/4 & -1/4 & 1/4 & 3/4 \end{bmatrix} \begin{bmatrix} \theta_1 \\ \theta_2 \\ \theta_3 \\ \theta_4 \end{bmatrix} \quad (6)$$

It can be seen from the above relationship that an identity matrix between $[\ \Delta\theta_1, \Delta\theta_2, \Delta\theta_3, \Delta\theta_4\ ]^T$ and $[\ \theta_1,\ \theta_2,\ \theta_3,\ \theta_4\ ]^T$ is not present in general. The two vectors in Equation (6) will be identical if ($\Delta\theta_1$ and $\Delta\theta_3$) and (θ_2 and θ_4) have the same magnitude and are always 180 degree out-of-phase with each other. A simulation study with the Black Hawk GENHEL model was conducted and the result is depicted in Figure 6.1 The equivalent blade root pitch motion due to IBC generated through the swash plate, $\Delta\hat{\theta}_1$, is reasonably close to the original direct IBC motion, $\Delta\theta_1$, in rotating frame. Given the complexity in mounting the

actuators directly on the blades and reliability considerations, IBC through swash plate is a practical way for implementation of IBC.

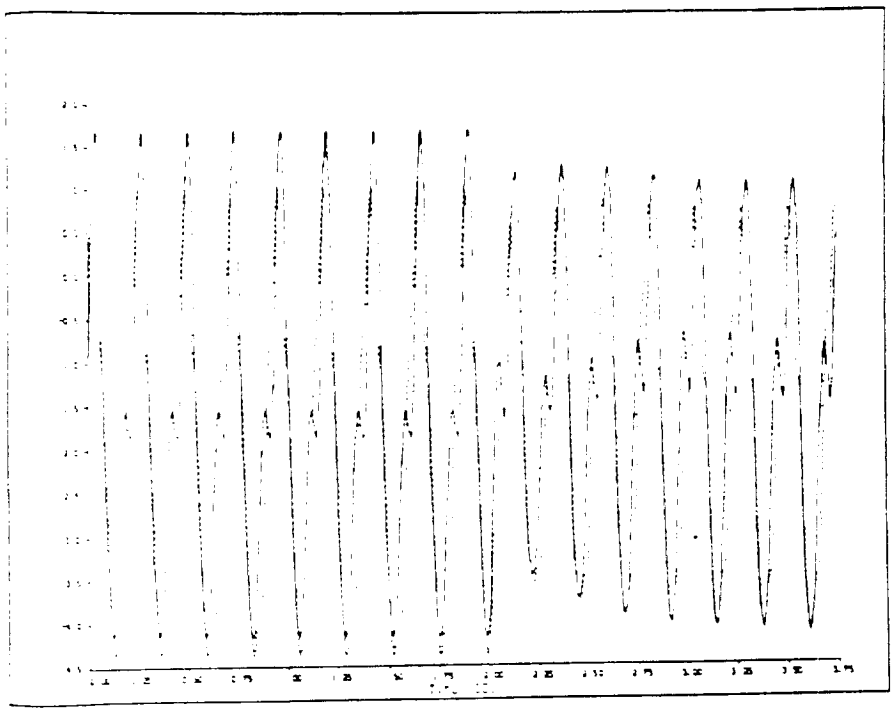

$\Delta\theta$ ——— : blade root pitch generated by direct IBC

$\Delta\hat{\theta}$ - - - - - - : blade root pitch generated by IBC via swash-plate motion

Figure 6.1 Blade root pitch motion

CHAPTER 7

GENERALIZED ROTOR STATES FEEDBACK CONTROL SYSTEM

In this chapter, a generalized rotor states feedback control system is defined. It is shown that the IBC system through swash plate control is a limited case of a general rotor states feedback control system[9].

The general coordinate transformation between blade flapping angles $\underline{\beta}_R$ in rotating frame and the rotor states $\underline{\beta}_{NR}$ in non-rotating frame is given by :

$$\underline{\beta}_R = T \; \underline{\beta}_{NR} \tag{1}$$

where

$$T = \begin{bmatrix} 1 & C\phi_1 & S\phi_1 & -1 \\ 1 & -S\phi_1 & C\phi_1 & 1 \\ 1 & -C\phi_1 & -S\phi_1 & -1 \\ 1 & S\phi_1 & -C\phi_1 & 1 \end{bmatrix}$$

$\underline{\beta}_R = [\ \beta_1,\ \beta_2,\ \beta_3,\ \beta_4,\ ]^T$ in rotating frame

$\underline{\beta}_{NR} = [\ \beta_0,\ \beta_{1c},\ \beta_{1s},\ \beta_{\frac{1}{2}}\ ]^T$ in non-rotating frame

$$\beta_i = \beta_0 + \beta_{1c} \cos\phi^i + \beta_{1s} \sin\phi_i + \beta_{\frac{1}{2}} (-1)^i$$

for i = 1, 2, 3, 4

Generalized pure IBC

For Ham's pure IBC system, individual root pitch angle vector $\Delta\underline{\theta}_{ibc}$ is generated from the blade states $[\ \underline{\beta}_R\ \dot{\underline{\beta}}_R\ \ddot{\underline{\beta}}_R\ ]$ using sensors mounted on the rotor blades. The control is performed in the rotating frame through actuators attached to the blade roots. The control law is given as

$$\Delta \underline{\theta}_{ibc} = K_1 \ddot{\underline{\beta}}_R + K_2 \dot{\underline{\beta}}_R + K_3 \underline{\beta}_R \quad (2)$$

Equation (1) is differentiated twice to give

$$\dot{\underline{\beta}}_R = \dot{T} \underline{\beta}_{NR} + T \dot{\underline{\beta}}_{NR} \quad (3)$$

$$\ddot{\underline{\beta}}_R = \ddot{T} \underline{\beta}_{NR} + 2\dot{T} \dot{\underline{\beta}}_{NR} + T \ddot{\underline{\beta}}_{NR} \quad (4)$$

Equation (2) is now written in terms of the non-rotating rotor state vector $\underline{\beta}_{NR}$ and its derivatives as

$$\begin{aligned} \Delta \underline{\theta}_{ibc} = {} & [K_1 \ddot{T} + K_2 \dot{T} + K_3 T] \underline{\beta}_{NR} + \\ & [2K_1 \dot{T} + K_2 T] \dot{\underline{\beta}}_{NR} + \\ & [K_1 T] \ddot{\underline{\beta}}_{NR} \end{aligned} \quad (5)$$

Equation (5) shows a pure IBC concept through the root pitch actuators control is a special case of the rotor states feedback control system with time-varying feedback gain vector as given in Equation (5).

Generalized IBC Concept via Swash plate Feedback

For a helicopter with 3 or 4 blades, the IBC control can be realized through the swash plate motion. Using Equation (1)

Since $\Delta \underline{\theta}_{ibc} = T \underline{\theta}_{swp}$

therefore $\Delta \underline{\theta}_{swp} = T^{-1} \underline{\theta}_{ibc} \quad (6)$

$$\begin{aligned} \Delta \underline{\theta}_{swp} = {} & T^{-1}[K_1 \ddot{T} + K_2 \dot{T} + K_3 T] \underline{\beta}_{NR} + \\ & T^{-1}[2K_1 \dot{T} + K_2 T] \dot{\underline{\beta}}_{NR} + \\ & T^{-1}[K_1 T] \ddot{\underline{\beta}}_{NR} \end{aligned} \quad (7)$$

This is equivalent IBC via rotor state feedback in the non-rotating frame through the swash plate motion. Now, consider a simplified case where the control law in Equation (2) is given as :

$$K_1 = k_1 I_4, \qquad K_2 = k_2 I_4, \qquad K_3 = k_2 I_4$$

Here k_1, k_2 and k_3 are scalar feedback gains and I_4 is an 4 x 4 matrix. With this simplified control logic, Equation (7) becomes :

$$\Delta \underline{\theta}_{swp} = [k_1 T^{-1}\ddot{T} + k_2 T^{-1}\dot{T} + k_3 I_4]\, \underline{\beta}_{NR} + [2k_1 T^{-1}\dot{T} + k_2 T^{-1}T]\, \dot{\underline{\beta}}_{NR} + [k_1 I_4]\, \ddot{\underline{\beta}}_{NR}$$

$$\Delta \underline{\theta}_{swp} = \begin{bmatrix} k_3 & 0 & 0 & 0 \\ 0 & k_3 - k_1\Omega^2 & k_2\Omega & 0 \\ 0 & -k_2\Omega & k_3 - k_1\Omega^2 & 0 \\ 0 & 0 & 0 & k_3 \end{bmatrix} \underline{\beta}_{NR} + \begin{bmatrix} k_2 & 0 & 0 & 0 \\ 0 & k_2 & 2k_1\Omega & 0 \\ 0 & -2k_1\Omega & k_2 & 0 \\ 0 & 0 & 0 & k_2 \end{bmatrix} \dot{\underline{\beta}}_{NR} + \begin{bmatrix} k_1 & 0 & 0 & 0 \\ 0 & k_1 & 0 & 0 \\ 0 & 0 & k_1 & 0 \\ 0 & 0 & 0 & k_1 \end{bmatrix} \ddot{\underline{\beta}}_{NR} \quad (8)$$

Note only first three control signals (elements) in $\Delta\underline{\theta}_{swp}$ are used for gust control.

For another special case where $K_1 = K/\Omega^2$, $K_2 = K/\Omega^2$ and $K_3 = K$, Equation (7) becomes

$$\Delta\underline{\theta}_{swp} = [K/\Omega^2\ T^{-1}\ddot{T} + K/\Omega\ T^{-1}\dot{T} + K]\ \underline{\beta}_{NR} + [2K/\Omega^2\ T^{-1}\dot{T} + K/\Omega\ T^{-1}T]\ \dot{\underline{\beta}}_{NR} + K\ \ddot{\underline{\beta}}_{NR} \tag{9}$$

After the matrixes are expanded, Equation (8) becomes

$$\Delta\underline{\theta}_{swp} = K\begin{bmatrix} 1 & 0 & 0 & 0 \\ 0 & 0 & 1 & 0 \\ 0 & -1 & 0 & 0 \\ 0 & 0 & 0 & 1 \end{bmatrix}\underline{\beta}_{NR} + K/\Omega\begin{bmatrix} 1 & 0 & 0 & 0 \\ 0 & 1 & 2 & 0 \\ 0 & -2 & 1 & 0 \\ 0 & 0 & 0 & 1 \end{bmatrix}\dot{\underline{\beta}}_{NR}$$

$$+ K/\Omega^2\begin{bmatrix} 1 & 0 & 0 & 0 \\ 0 & 1 & 0 & 0 \\ 0 & 0 & 1 & 0 \\ 0 & 0 & 0 & 1 \end{bmatrix}\ddot{\underline{\beta}}_{NR} \tag{10}$$

The control shown in Equation (10) is the original IBC concept proposed by Ham. Comparing Equation (10) with Equation (5), it is clear that IBC control scheme suggested by Ham is a limited case of the rotor states feedback control system.

General Rotor State Feedback through the Swash plate Motion

All the discussions so far on IBC control do not consider the helicopter body. In fact, motion of the fuselage will affect rotor flapping and vice versa. The body of the helicopter is isolated from external disturbance because of stabilizing effect provided by the rotor, which acts as a gyroscope. If fuselage body states are available for feedback, more versatile gust alleviation control law can be formulated. Studies on IBC by J.C. Wang has found that a significant reduction on the body vertical acceleration caused by gust can be achieved by adding a body vertical acceleration feedback loop into the IBC system[9].

If $\underline{\beta}_{NR}$, $\dot{\underline{\beta}}_{NR}$, $\ddot{\underline{\beta}}_{NR}$ can be estimated from sensors mounted on the blade, a general gust control law can be developed by using rotor and body states feedback as

$$\Delta \underline{\theta}_{swp} = K_1 \ddot{\underline{\beta}}_{NR} + K_2 \dot{\underline{\beta}}_{NR} + K_3 \underline{\beta}_{NR} + K_4 \underline{X}_B + K_5 \dot{\underline{X}}_B$$

where the fuselage body state vector $\underline{X}_B$ is

$$\underline{X}_B = [u,q,w,v,p,r]^T$$

u,v,w : linear velocity

p,q,r : angular velocity

The optimal gain matrixes K_1 through K_5 for a given flight

condition can be derived for control law synthesis when the nine degree-of-freedom rotorcraft state dynamic equations become available.

CHAPTER 8

CONCLUSIONS

In modern day helicopters, flapping provides a means of orientating the rotor thrust vector for stability and control functions. Simulation studies were performed to get some insight into Ham's original IBC method of reducing blade flapping due to gust disturbance. Results show that for an IBC model with periodic coefficients and controller gains, up to 36% in gust alleviation can be achieved with a maximum feedback gain KA of 1.2. When a simplified model with constant coefficients and gains is used, the reduction is decreased to about 22% for the same value of KA.

It is desirable to have a control system which is less sensitive to the DC value of the input control. A MRIBC (Model Reference IBC) method is suggested for possible improvement of Ham's original IBC. The sensitivity to control input is lessened since differences in flapping states between the model and the plant, instead of the states, are employed for control law synthesis in MRIBC. The performance of this method matches very well with that of Ham's in both time-varying and time-invariant cases. The Model Reference IBC system, however, becomes unstable at KA = .75 and KA = 1.2 respectively for time-varying and constant math model.

For its insensitivity to flight conditions and simplicity of implementation, kinematic estimator is used to

reconstruct the states required for IBC feedback given only measurements of some of the states. Two algorithms for estimating both flapping angle, rate and acceleration from a single measurement of angle (Direct Flap Estimator) were investigated. While satisfactory tracking of angle and rate can be attained, both procedures do not provide a good estimation on flapping acceleration. There appears to be a phase lag between the true and the estimated acceleration. The IBC Kinematic Estimator method utilizes two accelerometers attached to different locations on the blade to extract both flapping angle and angular acceleration information. Algorithm is then used to estimate flapping angular rate via a kinematic observer. This technique provides good estimations of all three states used for IBC control law synthesis. The method assumes that the blade motion is due to rigid body flapping.

The control for IBC can be exercised in the rotating frame by directly attaching actuators to the rotor blades. This mechanism, though appealing because of its simplicity, place severe demands on the actuators. It is shown that IBC can be achieved through a swash plate in the non-rotating frame when the control degrees-of-freedom equals to the number of blades. This is the case for a three bladed helicopter. When the number of blades is four, coordinate transformation can still be utilized to find an equivalent swash plate feedback control. A simulation study with GENHEL

shows blade root pitch motion generated by IBC via swash plate motion is reasonably close to that produced by direct IBC in the rotating frame.

Also presented in the thesis is the general rotor states feedback control system in the non-rotating reference frame. Ham's IBC system is shown to be a special case of the general rotor states feedback scheme. The optimum state feedback gains in Equation 7.11 can be found for higher gust alleviation. This is beyond the scope of this thesis, and is not further pursued here.

REFERENCE

[1]Prouty, R.W. Practical Helicopter Aerodynamics, Rotor & Wing International, 1982.

[2]Ham, N.D., Helicopter Individual Blade Control and Its Application, Proceedings 39th American Helicopter Society Annual Forum, 1987.

[3]Chen, T.N., Effects of Primary Rotor Parameters on Flapping Dynamics, NASA T P-1431, 1980.

[4]Johnson, W., Helicopter Theory, Princeton University press, Princeton University, New Jersey, 1980.

[5]Hohenemser, K.H. and Yim, S.K., Some Application of the Method of Multi-blade Coordinates, Journal of the American Helicopter Society, Vol. 17, NO 3, 1972.

[6]McKillip, R.M., Periodic Control of the Individual-Blade-Control Helicopter Rotor, 10th European Rotorcraft Forum, August, 1984, The Netherlands.

[7]DuVal, R.W., Use of Multiblade Sensors for On-line Rotor Tip-Path Plane Estimation, Journal of the American Helicopter Society, Vol. 25, NO 4, 1980.

[8]McKillip, R.M., Kinematic Observers for Rotor Vibration Control, the 42nd American Helicopter Annual Forum, 1986.

[9]Wang, J.C. and Talbot, P.D., Analysis and Computer Simulation of Individual Blade Control Concepts, NASA Progress Report, Feb., 1987.

[10]Franklin, G.F. and Powell, J.D., Digital Control of Dynamics System, Addison-Wesley Publishing Company, June, 1981.

APPENDIX

APPENDIX A

Derivation of Ham's IBC method

The flapping equation of motion is described by :

$$\ddot{\beta} + A(\mu,\phi)\dot{\beta} + B(\mu,\phi)\beta = C(\mu,\phi)\theta + W_g(\mu,w,\Omega) \qquad (1)$$

For the UH-60 blade used in the simulation, the parameters are given as :

$A = 23.76 + 31 * \mu * \sin\phi$

$B = 734 + (692.24 + 1323.8 * \mu * \sin\phi) * \mu * \cos\phi$

$C = 684.3 + (1808 + 1313 * \mu * \sin\phi) * \mu * \sin\phi$

$W_g = K_g (972 * \sin wt + 792 * \mu (\cos(\Omega-w)t - \cos(\Omega+w)t))$

$\theta_{swp} = 0.2975 + 0.009 * \cos \Omega t - 0.142 \sin \Omega t$

$\mu = 0.18$

$\Omega = 24$ rad/second

$w = 13$ rad/second

Here, the total blade root-pitch angle is consisted of two parts :

$$\theta = \theta^{*}_{swp} + \theta_{ibc}$$

where θ^*_{swp} is the effective blade pitch input due to motion of the swash plate, and θ_{ibc} is the individual pitch feedback control signal for gust alleviation.

The feedback control law is generated as :

$$\theta_{ibc} = (KA\ \ddot{\beta}/\Omega^2 + KR\ \dot{\beta}/\Omega + KP\ \beta) \qquad (2)$$

where K's are feedback control gains and

$$\theta^*_{swp} = K_{swp} * \theta_{swp} \qquad (3)$$

K_{swp} is the forward controller gain. Substituting Equations (2) and (3) into Equation (1), we obtain

$$\ddot{\beta} + \left(\frac{A + C\ KR/\Omega}{1 + C\ KA/\Omega^2}\right)\dot{\beta} + \left(\frac{B + C\ KP}{1 + C\ KA/\Omega^2}\right)\beta =$$

$$\left(\frac{C}{1 + C\ KA/\Omega^2}\right) K_{swp}\ \theta_{swp} + \left(\frac{1}{1 + C\ KA/\Omega^2}\right) W_g \qquad (4)$$

To reduce the gust effect acting upon the rotor blade, the controller gains can be selected such that the closed-loop blade dynamics equation will assume the form

$$\ddot{\beta} + A(\mu,\phi)\dot{\beta} + B(\mu,\phi)\beta = C(\mu,\phi)\theta_{swp} + 1/KG\ W_g$$

The controller gains are assigned as :

$$KR = KA * A/\Omega$$

$$KP = KA * B/\Omega^2$$

$$K_{swp} = 1 + C * KA/\Omega^2$$

$$KG = 1 + C * KA/\Omega^2$$

For Ham's simplified IBC scheme, the following assumption are made :

$$A \approx \Omega \quad ; \quad B \approx \Omega^2 \quad ; \quad C \approx \Omega^2$$

With the above simplification, the controller gains become

$$KR = KP = KA$$

$$K_{swp} = KG = 1 + KA$$

The IBC feedback control law is now

$$\theta_{ibc} = (\ddot{\beta} /\Omega^2 + \dot{\beta} /\Omega + \beta) \, KA$$

APPENDIX B

Derivation of Model Reference IBC method

To design a IBC control law which is less sensitive to the DC value of the blade flapping motion, a Model Reference IBC system is studied. Flapping equation of motion is given as :

$$\ddot{\beta} + A(\mu,\phi)\dot{\beta} + B(\mu,\phi)\beta = C(\mu,\phi)\theta + W_g(\mu,w,\Omega) \qquad (1)$$

where

$$\theta = \theta_{swp} + \theta_{ibc} \qquad (2)$$

If a math model of the blade is known,

$$\ddot{\beta}_m + A(\mu,\phi)\dot{\beta}_m + B(\mu,\phi)\beta_m = C(\mu,\phi)\theta_{swp} \qquad (3)$$

then the error in flapping angle can be formed by

$$e(t) = \beta(t) - \beta_m(t)$$

$\beta(t)$ is the measured angle, and $\beta_m(t)$ is the model response. From Equations (1) and (3), we have the error dynamics equation :

$$\ddot{e} + A(\mu,\phi)\dot{e} + B(\mu,\phi)e = C(\mu,\phi)\theta_{ibc} + W_g(\mu,w,\Omega) \qquad (4)$$

A control law can be generated as

$$\theta_{ibc} = (KA\ \ddot{e}/\Omega^2 + KR\ \dot{e}/\Omega + KP\ e) \qquad (5)$$

where

$$KR = KA * A/\Omega$$

$$KP = KA * b/\Omega^2$$

Substituting KR and KP, Equation (5) is now given as

$$\theta_{ibc} = KA/\Omega^2\ (\ \ddot{e} + A(\mu,\phi)\dot{e} + B(\mu,\phi)e\ ) \qquad (6)$$

Equation (4) becomes

$$\ddot{e} + A(\mu,\phi)\dot{e} + B(\mu,\phi)e = \frac{1}{1 + KA\ C/\Omega^2}\ W_g \qquad (7)$$

Equation (1) is now

$$\ddot{\beta} + A(\mu,\phi)\dot{\beta} + B(\mu,\phi)\beta = C(\mu,\phi)\theta_{swp} + \frac{1}{1 + KA\ C/\Omega^2}\ W_g \qquad (8)$$

From Equation (8) and Equation (4) of Appendix A, both control schemes reduce the effective gust level by a factor of 1 / (1 + KA (C/Ω^2)). MRIBC is dependent only on the

error signal e, $\dot{e}$ and $\ddot{e}$. It is less sensitive to the DC value of the flapping motion.

From a point of view of practical application, it is desirable to have constant coefficients in the blade flapping math model. Using the same approximations as in Appendix A,

$$A \approx \Omega \quad ; \quad B \approx \Omega^2 \quad ; \quad C \approx \Omega^2$$

Equation (3) becomes

$$\ddot{\beta}_m + \Omega \dot{\beta}_m + \Omega^2 \beta_m = \Omega^2 \theta_{swp} \tag{9}$$

and the control law is

$$\theta_{ibc} = KA \left(\ddot{e}/\Omega^2 + \dot{e}/\Omega + e \right) \tag{10}$$

APPENDIX C

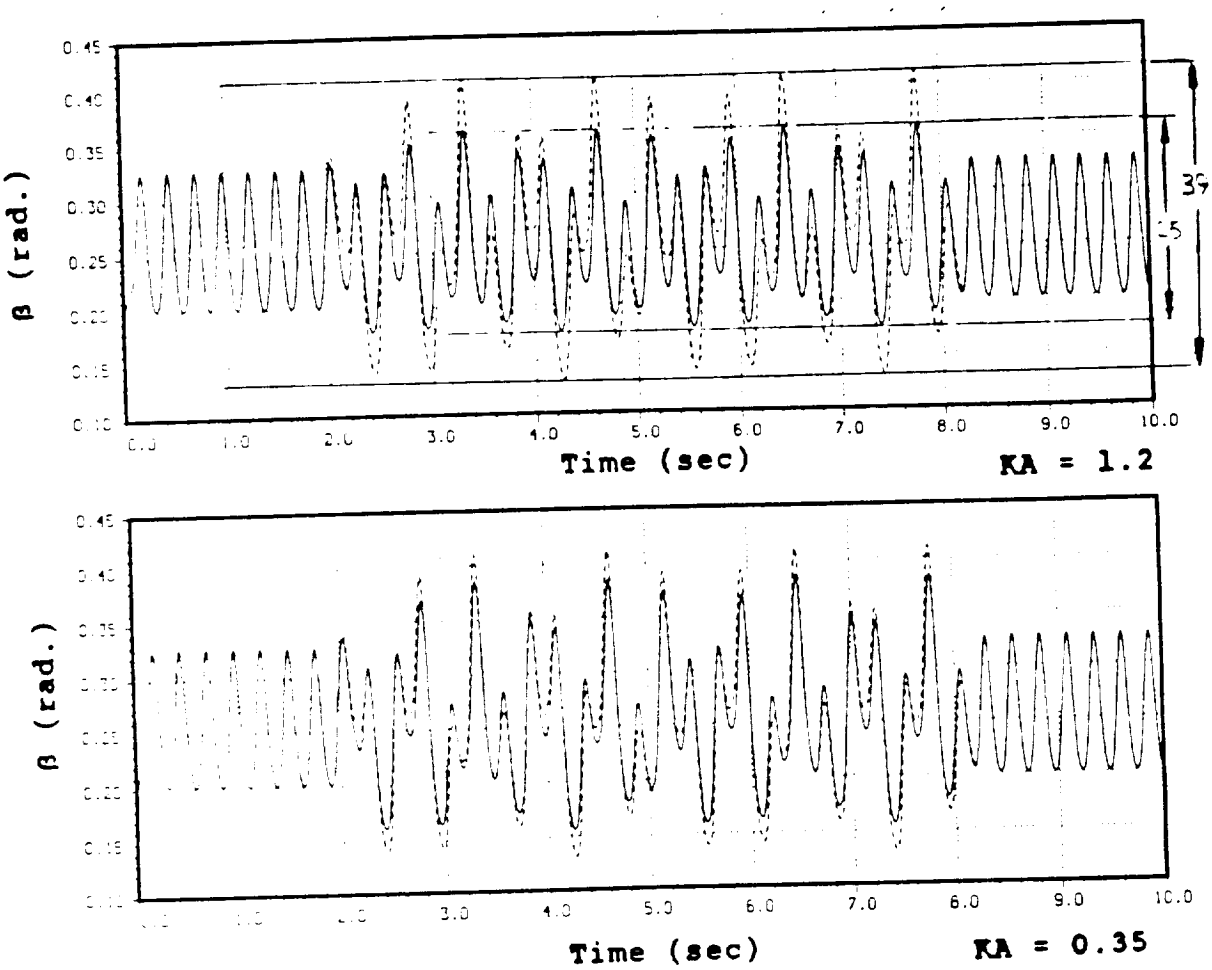

Open loop - - - - - - -

IBC in effect ————————

Figure 4.1 Gust alleviation vs controller gain KA

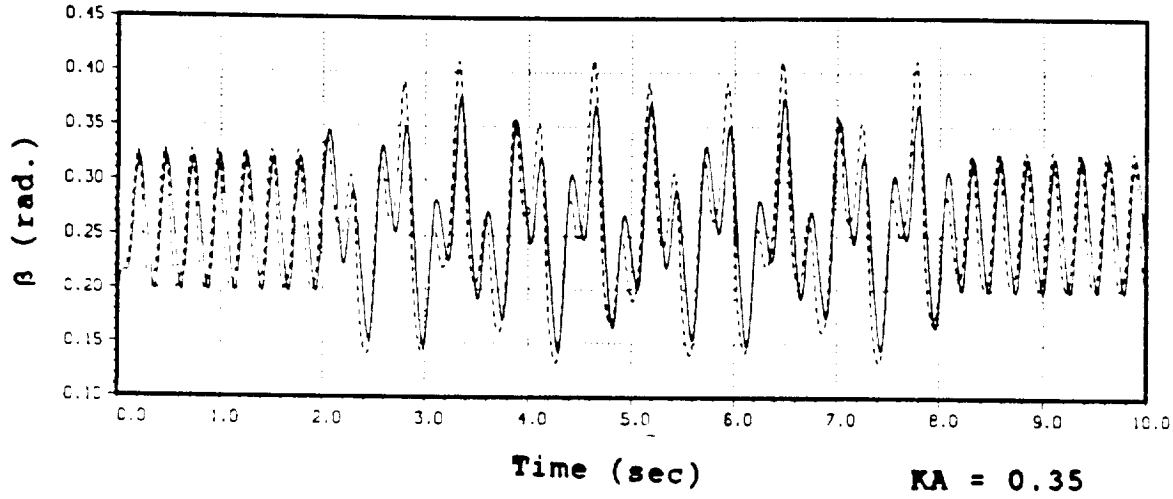

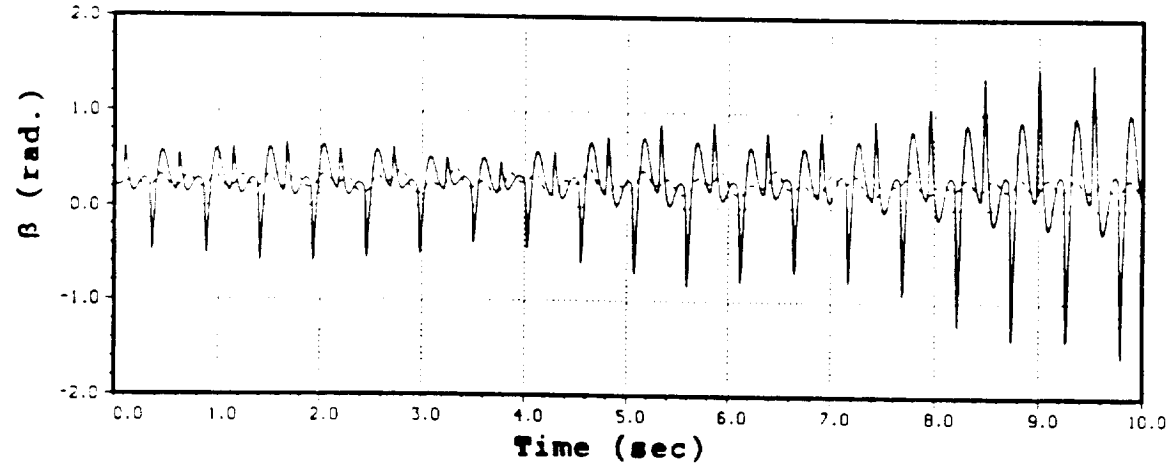

Figure 4.2 IBC second approach

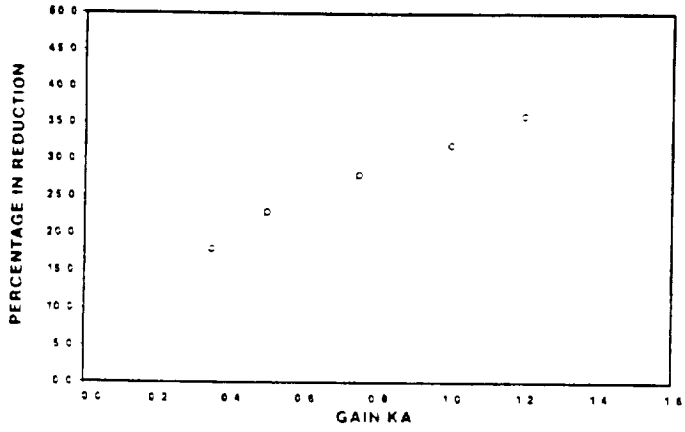

Figure 4.3 IBC performance, Ham's with time-varying gains

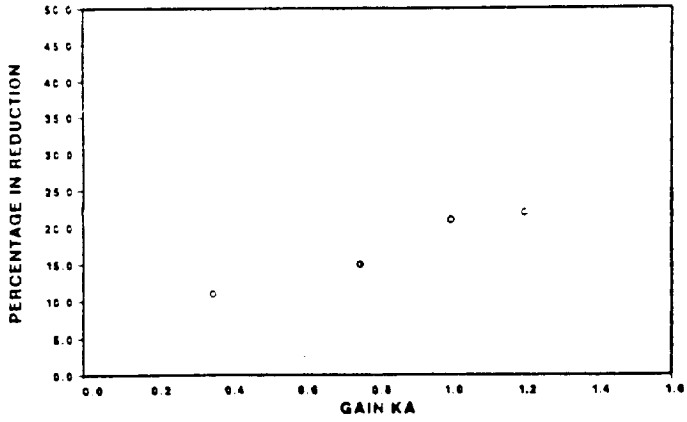

Figure 4.4 IBC performance, Ham's with time-invariant gains

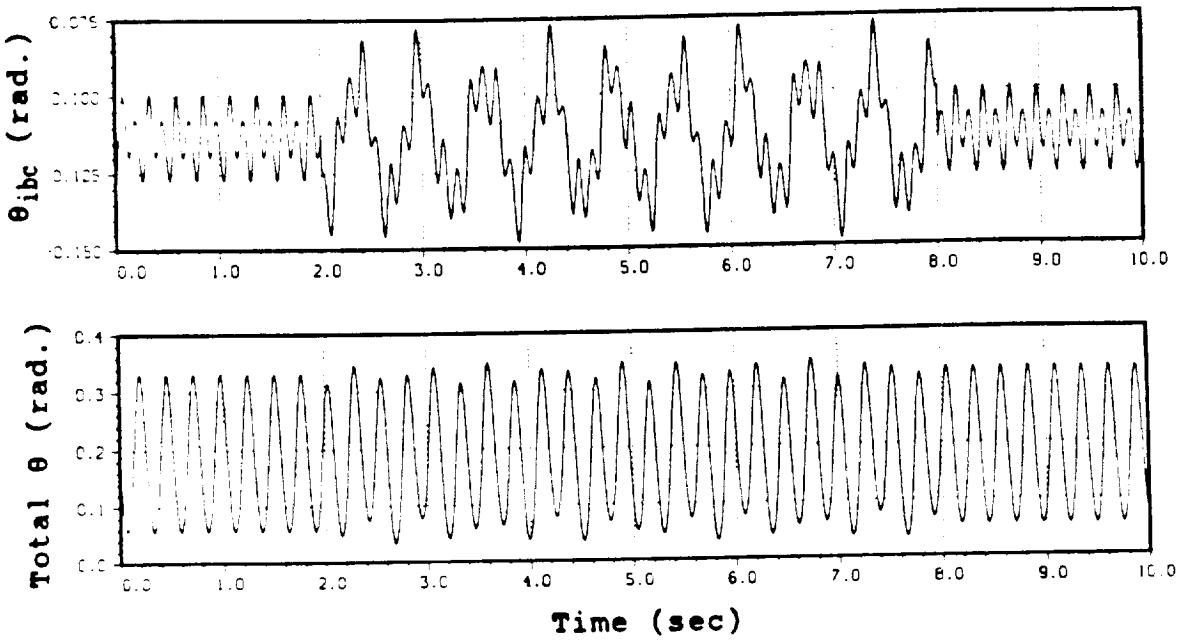

Figure 4.5 Control input for small gain KA

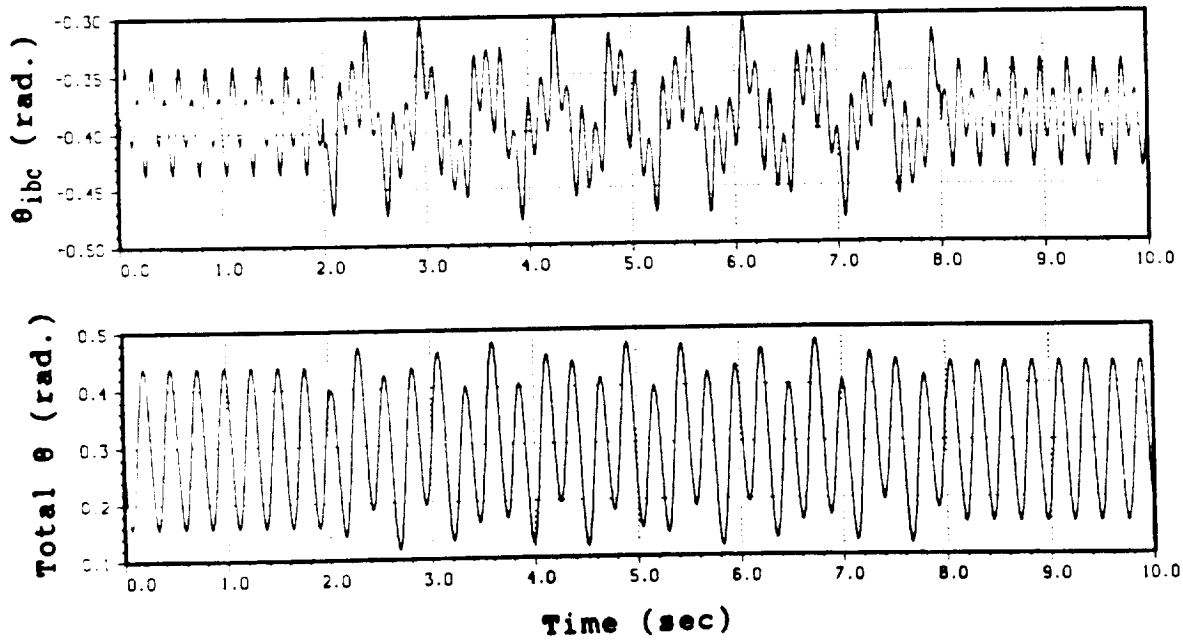

Figure 4.6 Control input for large gain KA

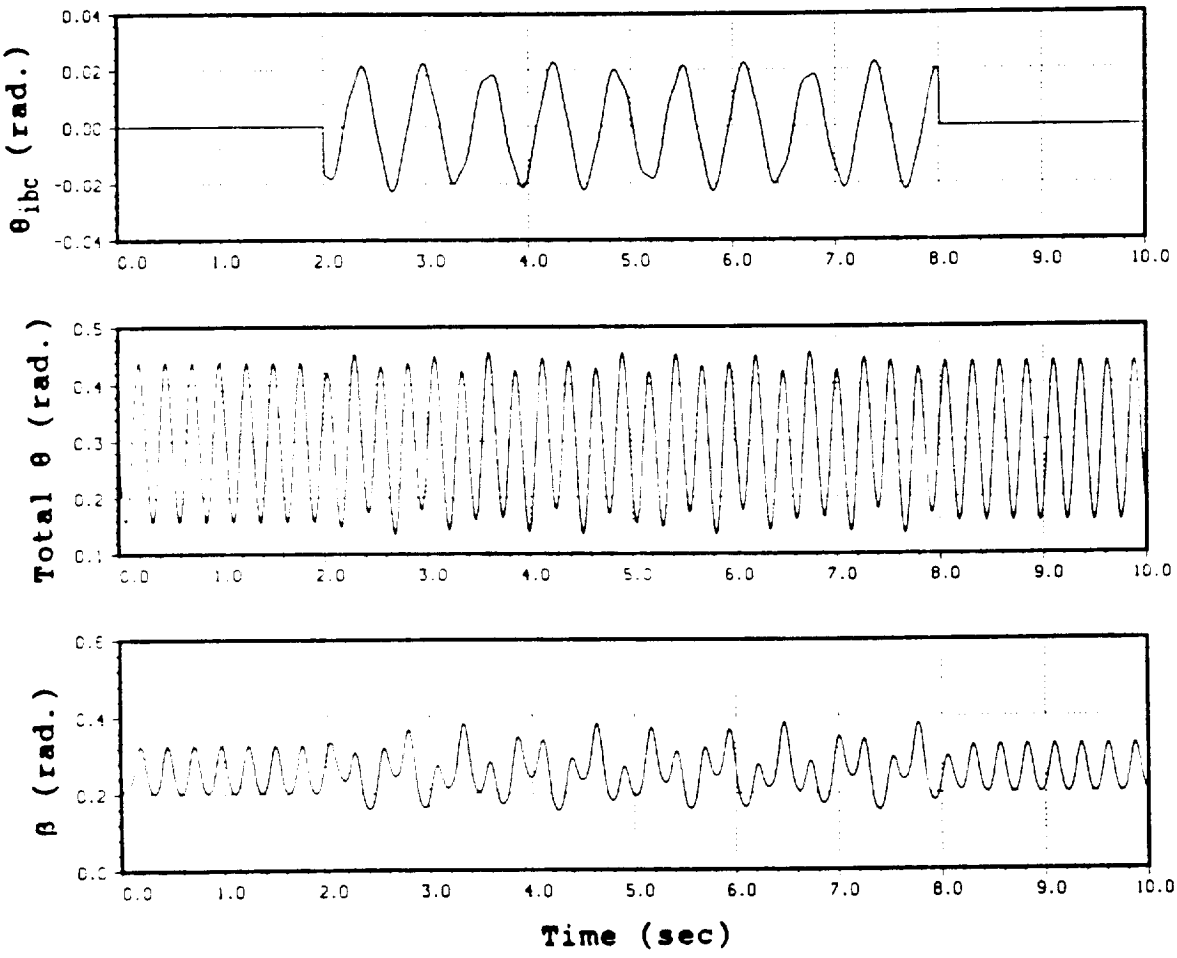

Figure 4.7 Model Reference IBC

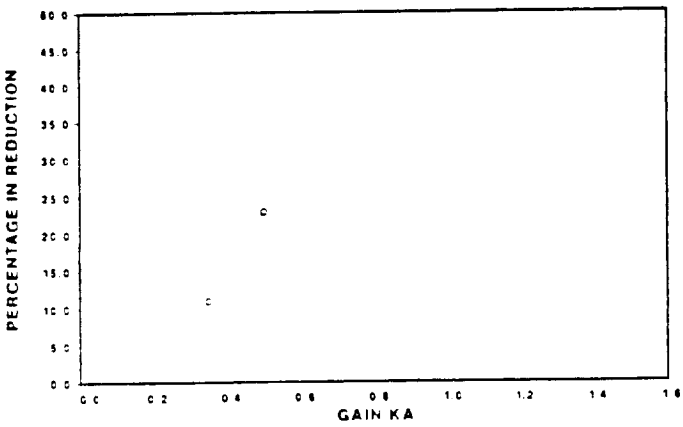

Figure 4.8 IBC performance, MRIBC with time-varying gains

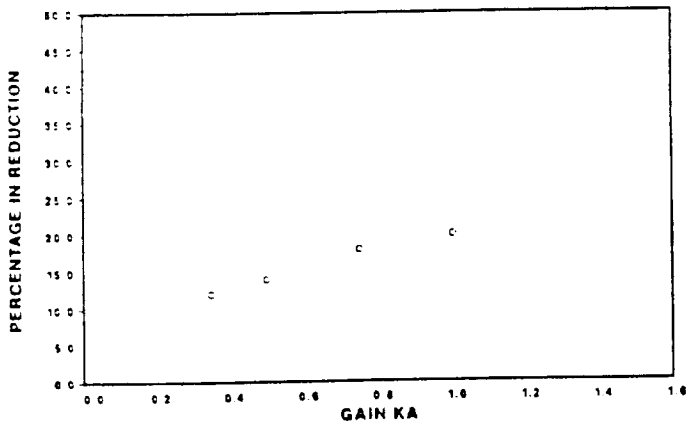

Figure 4.9 IBC performance, MRIBC with time-invariant gains

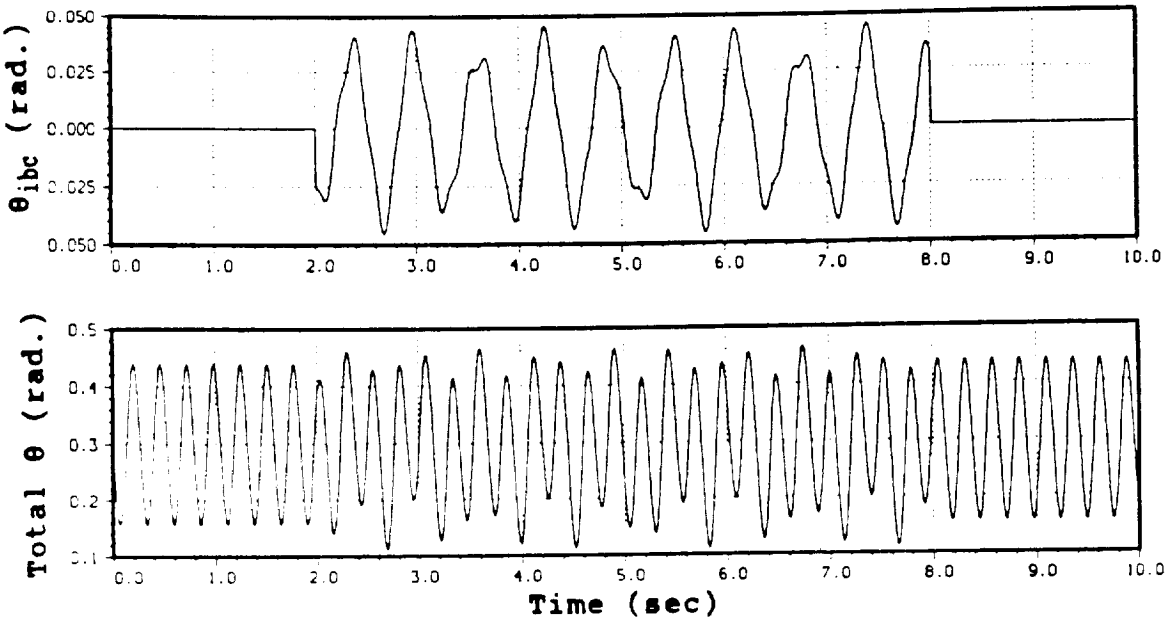

Figure 4.10 Sensitivity of control input to gain, IBC

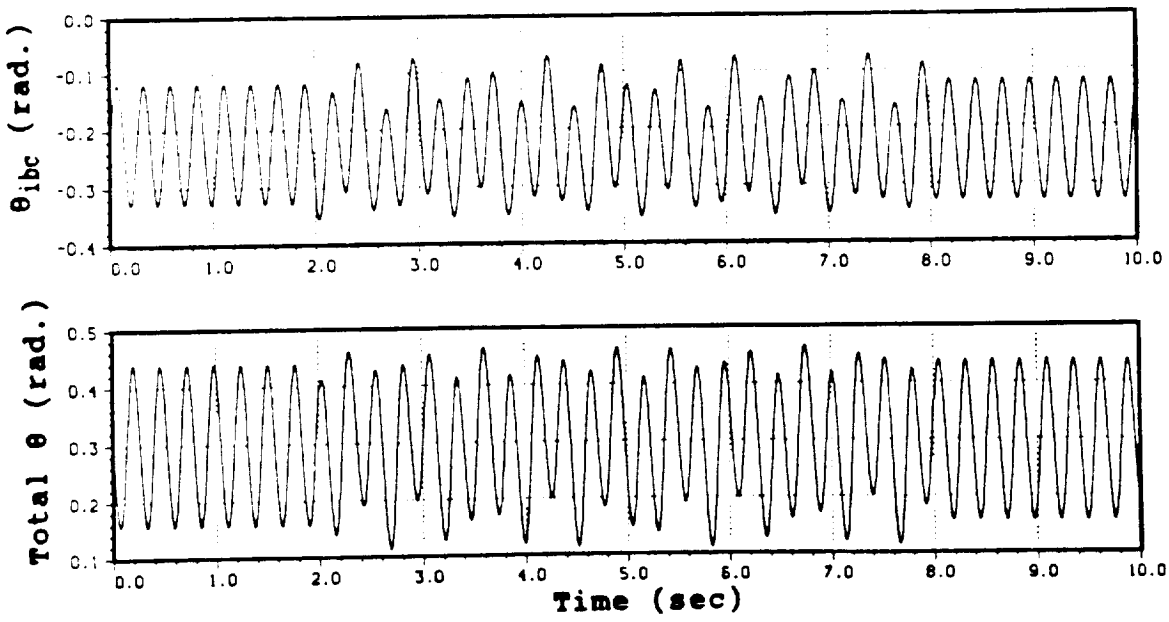

Figure 4.11 Sensitivity of control input to gain, MRIBC

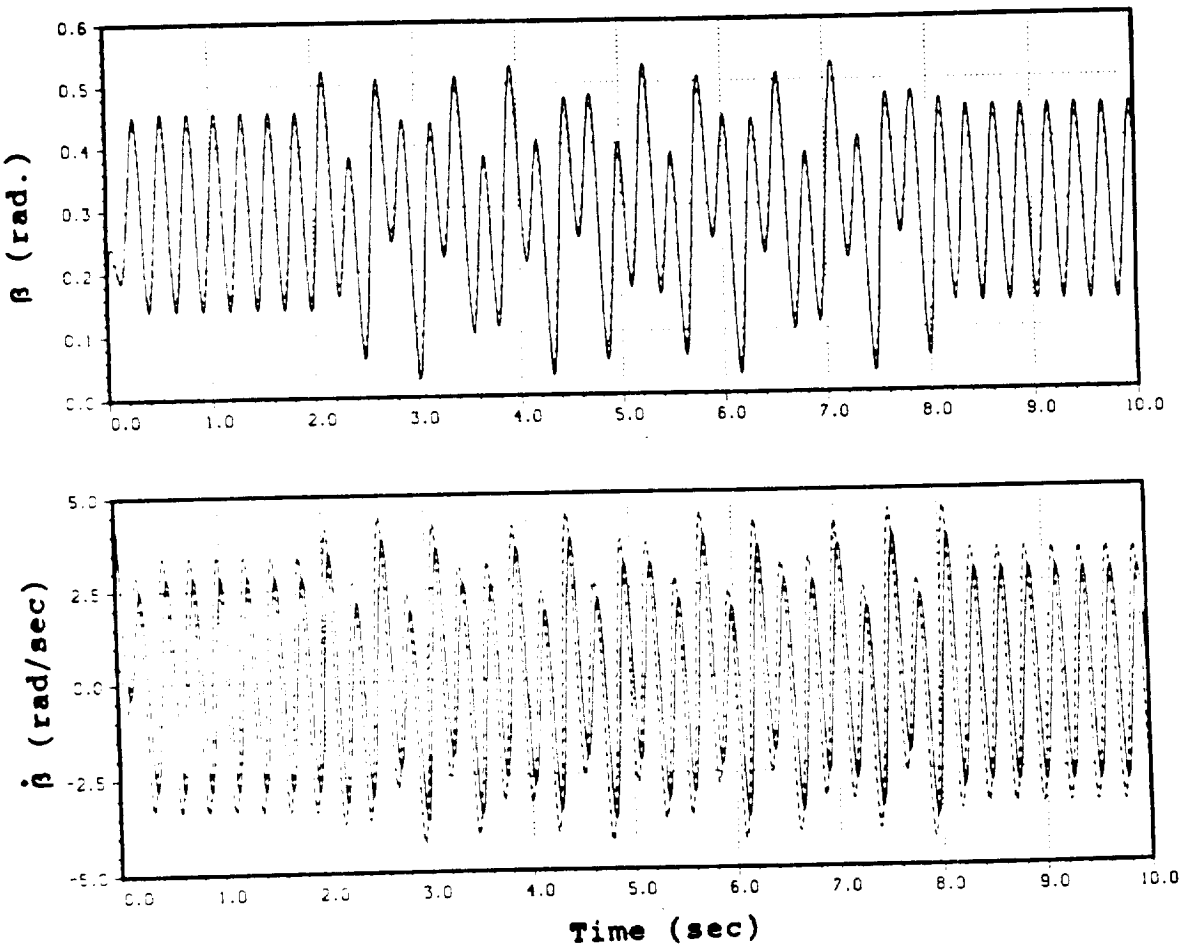

Figure 5.2 Direct Flap Estimator, with plant dynamics

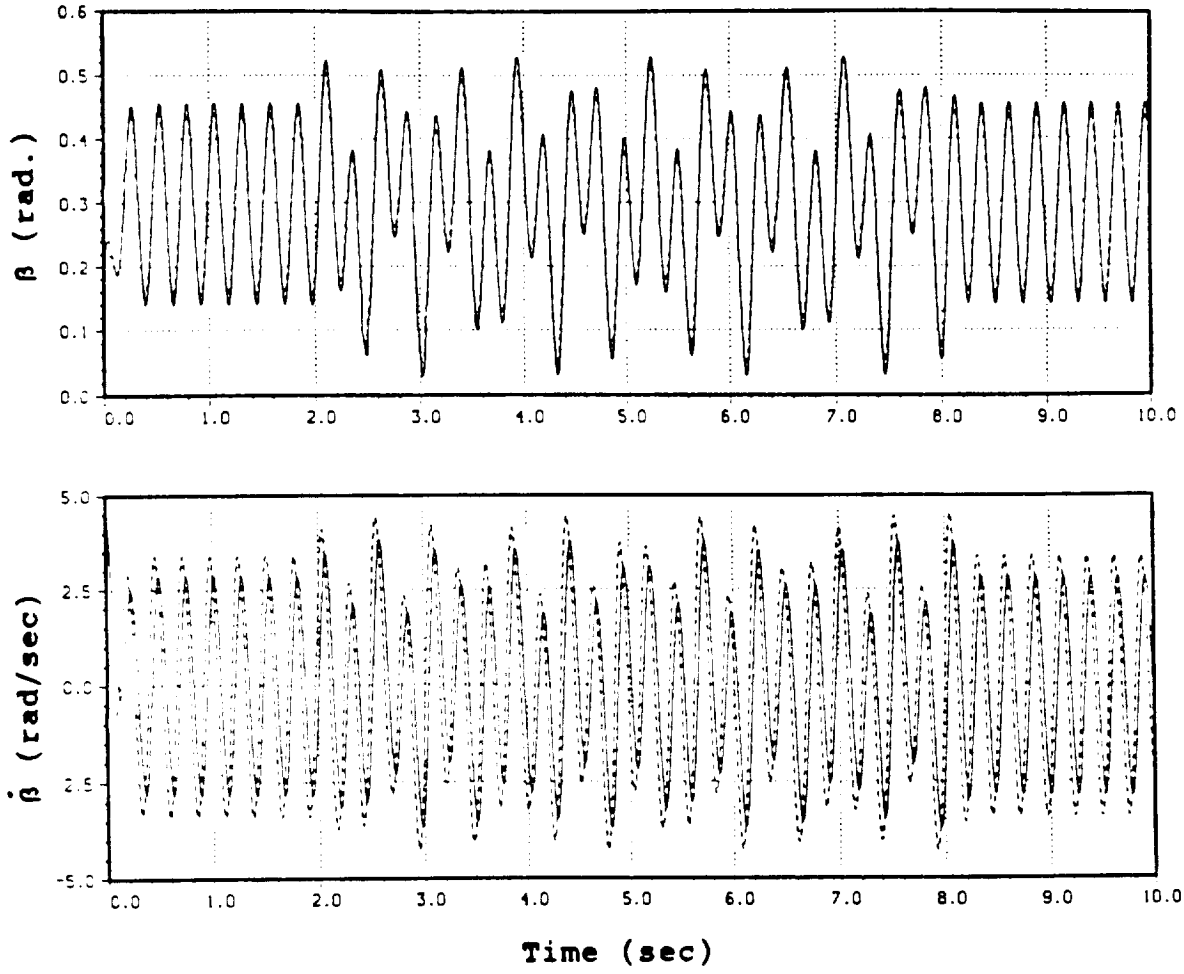

Figure 5.3 Direct Flap Estimator, no plant dynamics

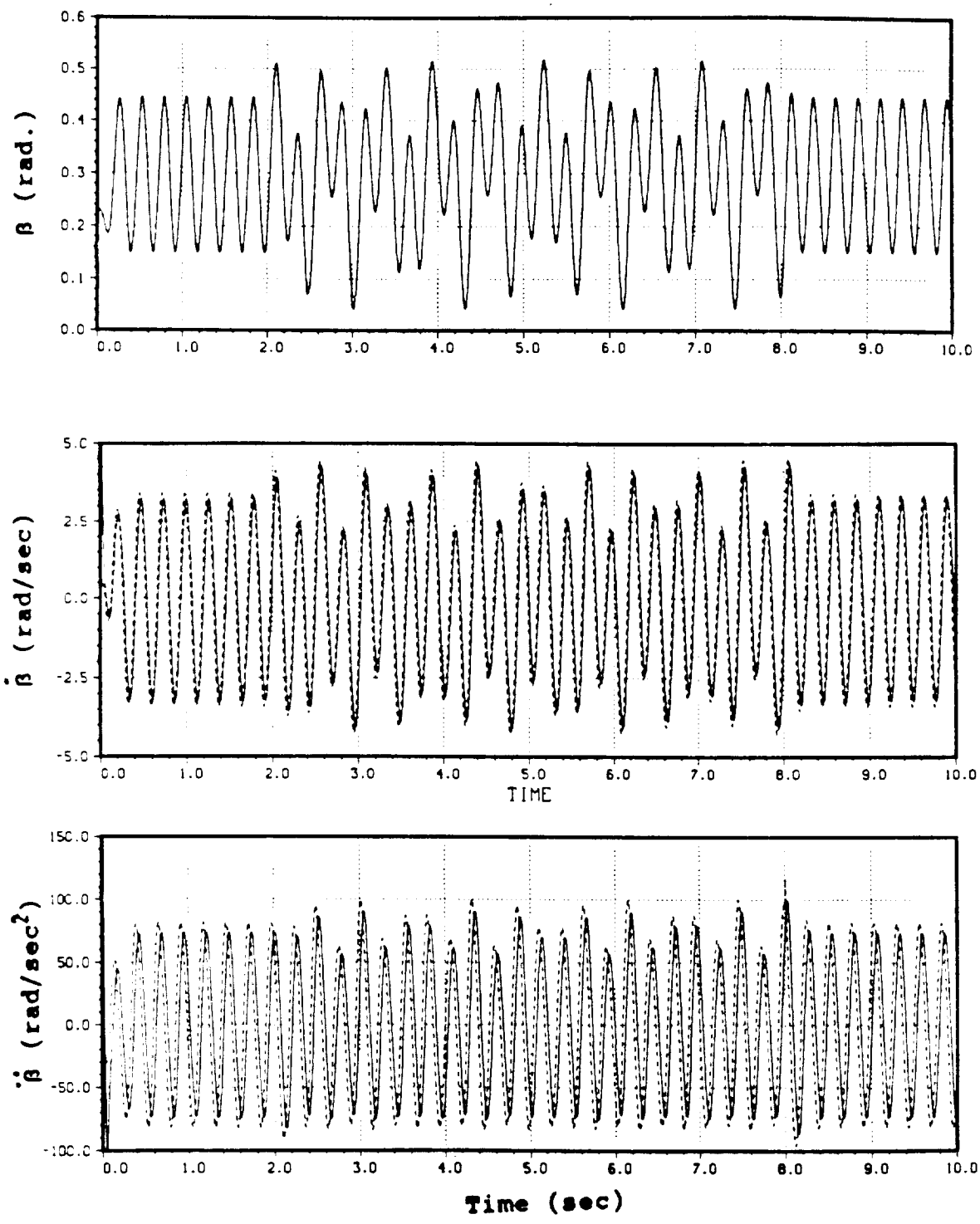

Figure 5.5 Cascaded Direct Flap Estimator

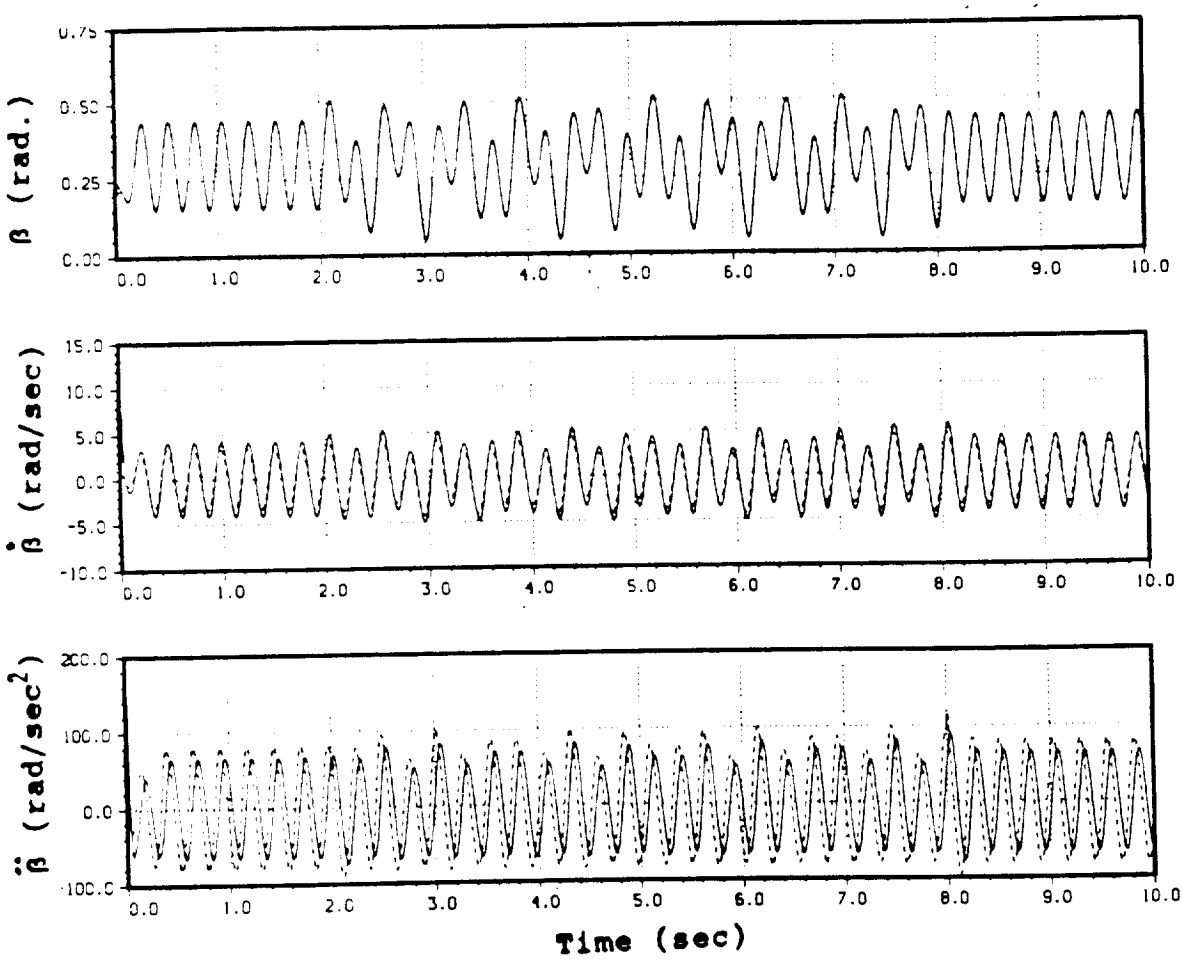

Figure 5.6 3 state Direct Flap Estimator

ACKNOWLEDGEMENT

This report is the MS thesis of Mr. A.Y.Chu , the department of Mechanical Engineering, San Jose State University (SJSU).

A preliminary study on the feasibility of Ham's IBC concept with a Black-Hawk helicopter simulation model had been performed by the NASA and SJSU collaborators (P.D. Talbot and J.C.Wang), and a progress report was submitted to the FHI Brnach. Chu and Wang have performed more indepth study on the IBC concept with the rotor system only. Their study are summarized in this report.

The IBC study with the GENHEL Black-Hawk model suggested that the blade states feedback alone is not sufficient for effective gust alleviation, the helicopter body states must also be fedback to improve handling quality of a vehicle under a gusty flight condition. The IBC concept is a limited case of the rotor states feedback control system. A more general rotor states feedback control system could be designed for gust control. We recommend more in-depth investigation of the flight measured data obtained from the Black-Hawk Phase 1 and Phase 2 flight tests. More extensive simulation study and also sensors and actuators investigation are also needed for a practical flight investigation of the IBC concept.

This study is partially supported by the NASA-SJSU cooperative program under the contract No.NCC-267.